University of Stavanger

Faculty of Science and Technology

MASTER'S THESIS

Study program/ Specialization: Petroleum Engineering/Drilling	Spring semester, 2014 Restricted access
Writer: **Benedicte Caroline Storebø**	…… (Writer's signature)

Faculty supervisor: Dr. Helge Hodne
Dr. Arild Saasen

External supervisors: Alexander Trondsen (Halliburton AS)
Elisabeth Balchen Gundersen (Halliburton AS)

Thesis title:

Gravel packing methods in long blank sections with near vertical regime in openhole

Credits (ECTS): 30

Key words: Sand control Openhole gravel packing Gravel settling Screen Boycott effect Blank pipe section Structural unit	Pages: ……85……. + enclosure: …… Stavanger, June 16, 2014

GRAVEL PACKING METHODS IN LONG BLANK SECTIONS WITH NEAR VERTICAL REGIME IN OPENHOLE

Benedicte Caroline Storebø

June 16, 2014

ACKNOWLEDGEMENTS

Work on this thesis has been exciting, challenging and particularly instructive. I have through this thesis gained a greater understanding of the completion subjects taken at the University of Stavanger. I am convinced that the new knowledge I have acquired during the work of this thesis will be beneficial for me in the years to come.

First and foremost I wish to thank my Faculty supervisor Dr. Helge Hodne, Associate Professor at UiS for his remarks and engagement on this thesis.

I would especially like to thank both Alexander Trondsen, Principal Engineer at the Sand Control Department and Elisabeth Balchen Gundersen, Account Representative in Sand Control and Business Development Production Enhancement at Halliburton, who gave me the opportunity to write this thesis, and for guiding me through it.

Furthermore, I would like to thank Dr. Arild Saasen at DetNorske/UiS. His expertise, experience and knowledge within the subject have been indispensable in helping me writing this thesis.

My mother, Ingvill Storebø deserves a big thanks for her support, discussions, proofreading and suggestions for structural improvements through this thesis. Last but not least, I would also mention friends and fellow students and thank them for coffee breaks, encouragement and motivation through 5 fantastic years at the University of Stavanger.

ABSTRACT

Gravel packing is a well-known method in sand control where stabilizing the formation with gravel prevents the production of formation sand. Longer and more complex completion operations are making the business of completing wells continually changing with new challenges, new technology and new methods.

The purpose of this thesis is to discuss the gravel placement in nearly vertical openhole systems with blank pipe sections between the screens. In vertical openhole completions with long blank pipe sections slurry and gravel settling regimes will occur differently compared to a conventional gravel pack operation without blank pipe sections. The reason for this is when a lower screen section is packed with gravel and the overlying section is with blank pipe, the carrier fluid can no longer flow through the lower screen. The gravel in the blank pipe sections is mainly settling due to gravitational forces and therefore displaces the carrier fluid, which flows upwards to the upper screen section. By simulating gravel pack operations with blank pipe sections in Halliburton's laboratory scale model in Tananger it has recently been shown (with continuous pumping) that with a higher inclination on the well (less vertical), a better packing is achieved in the blank pipe section; a higher gravel pack efficiency is achieved.

By analyzing and calculating theoretically how the gravel settles with regards to physical laws in fluid dynamics will give a better view on how to optimize the packing of gravel in the blank pipe sections in nearly vertical wells. How to optimize the packing in these blank pipe sections without the use of extensive expensive rig-time was one of several challenges that had to be taken into account during the work with this thesis. The combination of solids and fluid in one flow resulted in complex calculations, and certain parameters were therefore predetermined and assumptions like fluid loss and particle interaction were set to zero to simplify the calculations. The parameters in this thesis take the basis in ta field located in the Norwegian sector.

SYMBOLS AND NOMENCLATURE

1_{SU}	Structural unit number 1 in a line	
2_{SU}	Structural unit number 2 in a line	
3_{SU}	Structural unit number 3 in a line	
58_{SU}	Structural unit number 58 in a line	
A	Cross sectional area	L^2, m^2 (in^2)
A_{OH-BP}	Cross sectional area between open hole and base pipe	L^2, m^2 (in^2)
$A_{OH-Screen}$	Cross sectional area between open hole and screen	L^2, m^2 (in^2)
A’	Buzzelli friction factor equation segment	
B’	Buzzelli friction factor equation segment	
C_u	Uniformity Coefficient	
C_{BP}	Outer circumference of base pipe	L, m
C_{OH}	Circumference of openhole	L, m
d_{10}	Sand grain size at 10% cumulative level	L, µm (in)
d_{25}	Sand grain size at 25% cumulative level	L, µm (in)
d_{40}	Sand grain size at 40% cumulative level	L, µm (in)
d_{50}	Sand grain size at 50% cumulative level	L, µm (in)
d_{70}	Sand grain size at 70% cumulative level	L, µm (in)
d_{75}	Sand grain size at 75% cumulative level	L, µm (in)
d_{90}	Sand grain size at 90 % cumulative level	L, µm (in)
D	Diameter	L, m (in)
D_{BPI}	Inner diameter of base pipe	L, m (in)
D_{BP}	Outer diameter of base pipe	L, m (in)
D_{WP}	Outer diameter of washpipe	L, m (in)
D_{WPI}	Inner diameter of washpipe	L, m (in)
D_{OH}	Diameter of openhole	L, m (in)
D_S	Outer diameter of screen	L, m (in)
D_{SI}	Inner diameter of screen	L, m (in)
D_p	Particle diameter	L, µm (in)
D_H	Hydraulic diameter	L, m (in)
D_o	Outer diameter	L, m (in)
D_i	Inner diameter	L, m (in)
D_{10}	Gravel diameter size at 10% cumulative level	L, µm (in)
D_{40}	Gravel diameter size at 40% cumulative level	L, µm (in)
D_{50}	Gravel diameter size at 50% cumulative level	L, µm (in)
D_{70}	Gravel diameter size at 70% cumulative level	L, µm (in)
F_d	Frictional drag force	m L s^{-2}, N
F_g	Gravitational force	m L s^{-2}, N

f	Darcy-Weisbach friction factor	
g	Gravitational constant	L t^{-2}, m/s^2 /
h_L	Head loss	L, m (in)
h_w	Wire height	L, m (in)
h_{layer}	Height of one layer of structural units	L, m
K	Hydraulic conductivity	L s^{-1}, (m/s)
L	Characteristic length	L, m (in)
L_a	Additional settling length for a SU	L, m
m	Mass	m, kg
m_b	Mass of brine	m, kg
m_g	Mass of gravel	m, kg
m_{slurry}	Mass of slurry	m, kg
$\dot{m}_b$	Mass flow rate of brine	m t^{-1}, kg/min
$\dot{m}_g$	Mass flow rate of gravel	m t^{-1}, kg/min
$\dot{m}_{slurry}$	Mass flow rate of slurry	m t^{-1}, kg/min
n_{SU}	Structural unit number *n* in a line	
N_{Re}	Reynolds number	
N_{SU}	Number of structural units	
p	Wetted Perimeter	L, m (in)
P	Pressure	m L-1 s-2
Q	Flow rate	L^3 t^{-1}, m^3/min
Q_a	Flow rate in annulus	L^3 t^{-1}, m^3/min
Q_b	Brine rate	L3 t-1, m3/min
Q_g	Gravel rate	L^3 t^{-1}, m^3/min
Q_{ma}	Flow rate in mini-annulus	L^3 t^{-1}, m^3/min
Q_P	Pumping rate	L^3 t^{-1}, m^3/min
Q_p	Packing rate	L^3 t^{-1}, m^3/min
Q_{slurry}	Slurry rate	L^3 t^{-1}, m^3/min
r_p	Particle radius	L, m (in)
Re_p	Particle Reynolds number	
S_o	Sorting Coefficient	
t	Time	t, s
t_l	Time per layer for all layers except the first layer	t, s
t_n	Time until structural unit number *n* reaches length L	t, s
t_a	Additional time for a structural unit to settle	t, s
T_P	Pumping time	t, min
T_{P90}	Pumping time with gravel conc. of 90 kg/min	t, min
$T_{P123.537}$	Pumping time with gravel conc. of 123.537 kg/min	t, min
v_b	Velocity of brine	L t^{-1}, m/min

v_g	Velocity of gravel	L t^{-1}, m/min
v_p	Velocity of particle	L t^{-1}, m/min
v_s	Settling velocity	L t^{-1}, m/s
v_{SU}	Settling velocity of structural unit	L t^{-1}, m/s
v_{slurry}	Velocity of slurry	L t^{-1}, m/min
V_{bs}	Volume brine occupying open gravel pore space	L^3, m^3
V_{bs}	Volume brine flowing through upper screen	L^3, m^3
V_{DP}	Volume drillpipe	L^3, m^3
V_{fb}	Volume fraction brine	
V_{fbs}	Volume fraction brine flowing through upper screen	
V_{fpg}	Volume fraction packed gravel	
V_{fg}	Volume fraction gravel	
V_g	Volume gravel	L^3, m^3
V_{SU}	Volume structural unit	L^3, m^3
ε	Absolute roughness	L, m (in)
ε / d	Relative roughness	
ΔH	Difference in fluid potential in a medium	L, m (in)
$\Delta\rho$	Density difference between particle and fluid	m L^{-3}, kg/m^3
ΔP_f	Frictional pressure drop	m L^{-1} t^{-2}, bar (Pa)
$(\Delta P/L)_f$	Friction pressure gradient	m L^{-2} t^{-2}, bar/m (Pa/m)
$(\Delta P/L)_h$	Hydrostatic pressure gradient	m L^{-2} t^{-2}, bar/m (Pa/m)
Δt	Time difference	t, s
ρ_b	Density of brine	m L^{-3}, kg/m^3
ρ_f	Density fluid	m L^{-3}, kg/m^3
ρ_g	Density of gravel	m L^{-3}, kg/m^3
ρ_{gb}	Density of gravel bed	m L^{-3}, kg/m^3
ρ_{slurry}	Density of slurry	m L^{-3}, kg/m^3
μ	Viscosity	m L^{-1} t^{-1}, cp (kg/m-s)
μ_f	Carrier fluid viscosity	m L^{-1} t^{-1}, cp (kg/m-s)
θ	Inclination of well relative to the vertical direction	

ABBREVIATIONS

API	American Petroleum Institute
BP	Base Pipe
CLAM	Constant Level Additive Mixer
CH	Cased Hole
DST	Drill Stem Test
ECD	Equivalent Circulation Density
FEA	Finite Element Analysis
G-S	Gravel-Sand
HPHT	High Pressure High Temperature
HEC	Hydroxy-Ethylcelluse
LPS	Laser Particle Size
MD	Measured Depth
MSE	Mean Square Error
NCS	Norwegian Continental Shelf
OD	Outer Diameter
OH	Openhole
OHGP	Open Hole Gravel Pack
PE	Production Enhancement
PSD	Particle Size Distribution
RP	Recommended Practices
SAS	Stand Alone Screens
SG	Specific Gravity
SU	Structural Unit
TVD	True Vertical Depth
UiS	University in Stavanger
US	United States
WP	Washpipe
XC	Clarified Xanthum

TABLE OF CONTENTS

LIST OF FIGURES

LIST OF TABLES

LIST OF EQUATIONS

SI METRIC CONVERSION FACTORS

Convert from	To	Multiplication factor
Bar	Pascal (Pa)	1.0×10^{5}
Barrel	Cubic meters (m^3)	1.589873×10^{-1}
Centipoise (cp)	Pascal second (Pa-s)	1.0×10^{-3}
Degree Celsius	Kelvin (K)	$T_K = T_{°C} + 271.15$
Foot (ft)	Meter (m)	3.048×10^{-1}
Inch (in)	Meter (m)	2.54×10^{-2}
Pounds per gallon (ppg)	Grams per cubic centimeter (g/cm^3)	1.198×10^{-1}
Minute (min)	Seconds (s)	6.0×10^{1}

1. FOREWORD

A well-known and costly problem when producing oil and gas is related to the production of formation sand in unconsolidated sandstone reservoirs. As an important part of sand control in Norway gravel packing is one of several methods used to avoid the production of formation sand in a well. Depending on the formation several different gravel pack systems are available. The reservoirs on the Norwegian Continental Shelf (NCS) are mainly sandstone reservoirs, and an Openhole (OH) completion is then generally sufficient when it comes to both operational and economical aspects as the complexity and cost of perforating can be avoided.

In order to isolate the different zones in the reservoir and to reduce the cost of expensive screens, blank pipe sections are set between the producing zones in the well. Various methods of placing gravel in vertical wells with long blank sections have been applied in the field; batch pumping with various sizes and time between each batch has been tested without filling the entire blank section. In a conventional gravel pack operation it is always desirable to achieve a hundred percent pack efficiency, and this is of course desirable to achieve in wells with blank pipe sections as well.

Statoil have completed Openhole Gravel Pack (OHGP) operations with blank pipe sections successfully. However, in some cases of vertical/nearly vertical wells with blank pipe section between screens, theoretical calculations on pack efficiency have not reflected what actually happens in the field.

Statoil have in cooperation with Completion Tools and Productions Enhancement (PE) in Halliburton showed their interest regarding the process of gravel packing with long blank pipe sections in near vertical wells in OH completion. On Halliburton's scaled gravel pack model several tests have therefore been carried out, revealing a different gravel settling behaviour than earlier expected. This master thesis for the University of Stavanger (UiS) is a part of the investigation on the gravel settling behaviour that occurs. By investigating how these packing and settling regimes in blank pipe sections applies will give a better knowledge of how to assure an optimized gravel pack in the future.

2. SAND CONTROL

The fundamentals of sand control will be explained broadly in this chapter in order to give the reader information related to why and when a gravel pack operation is needed.

2.1 Introduction

One of the oldest problems faced by oil companies and one of the toughest one to solve is related to sand entering production wells.[1] Worldwide, approximately 70% of the oil and gas reserves are contained in poorly consolidated reservoirs where production of formation sand is likely to become a problem during the life of the field.[2] Sand control refers to managing and minimizing this formation sand and fines production during petroleum production, and with a fast growing industry in terms of technology are new and modified methods constantly developed to improve sand control. A study from February 2014 concerning sand control in High Pressure High Temperature (HPHT) environments concluded that gravel packing in HPHT environments is fully qualified, feasible and even more robust than the conventional Stand Alone Screens (SAS) that are traditionally used.[1, 3]

The production of sand can cause severe operational problems for the operators, and every year the petroleum industry spends millions of dollars on repairs and cleaning due to sand production, not to mention the lost revenues due to restricted production rates.[1]

In a sand control application the success or failure should always be measured against the three related criteria below:

- Maintain maximum well productivity
- Stop the production and movement of formation sand
- Pay for treatment costs and realize a satisfactory return on investment within a reasonable period of time[4]

2.2 Causes for sand production

The produced sand from a well can be divided into to types: sand fines and load-bearing sand particles, where the load-bearing ones are solids between 50 and 75 percentile ranges. The production of fines is normally unavoidable and can actually be beneficial when it comes to plugging of formation or gravel pack since they move around freely; the fines clean the pore space.[4, 5] When it comes to the production of load-bearing sand particles however, it is desirable to keep the sand production below an acceptable level at anticipated producing conditions and flow rates.[4]

The grains in the formation sand are stabilized due to capillary forces, frictional forces between grains, compressive forces by overburden weight, and cementation between the sand grains.[6] General causes for sand production are often related to the following factors:

- Reduced relative permeability: An increased saturation will result in a reduced relative permeability to oil, which again increases the pressure drawdown for a given production rate.[6]
- Drag forces: A higher fluid viscosity and/or a flow rate above the critical flow rate will result in an increase in the drag forces for the flowing fluid.[1, 6]
- Reduction in formation strength: The reduction in formation strength is often associated with water production/water breakthrough as the water dissolves or disperses the cementing materials that are holding the individual sand grains together. The sand will become unstable and sand production is then a factum. When water saturation increases, the capillary forces are reduced and this affects the compressive strength of the formation. Poorly consolidated sandstone formations are normally related to areas with a formation strength less than 1,000 psi.[1, 6, 7]
- Declining reservoir pressure: The cementation between the grains may be disturbed as declining reservoir pressure increases the completion forces.[6]

2.3 Consequences of sand production

A small quantity of formation sand can in many cases be produced without any significant adverse effects. However, without sand control the production of sand can cause several problems like reduced productivity, sand filled wells, erosion on equipment, downtime, and in worst case a complete loss of the productive zone or loss of well.[4, 8] Erosion and wear on equipment can lead to downtime and expensive repair, e.g. when sand accumulates in a separator it would result in fluid resident time and cause a poor performance of the separator. To restore the production efficiency of the well, the well needs to be shut-in and a manually cleaning of the separator is performed. This results in extra cost for the operator due to cleaning costs and not at least the cost of deferred production.[1, 8] Fig. 1 shows how production of sand can erode a wellhead piping.

Figure 1: An eroded wellhead piping[9]

By producing sand there are also problems related to the accumulation of sand on surface. This relates particularly to offshore locations where several wells often are tied up to the same platform; the amount of sand can then become quite large, and will take up too much space on the surface. On remote locations the deposition of sand will also cause an extra cost when the environmental consequences have to be considered.[4, 8]

2.4 Sand prediction and detection

In order to determine if sand control is required or not for a given geological area depends on the sanding potential prediction. When predicting the amount of formation sand that can and/or will be produced during production several methods are used: laboratory experiments, field observations and theoretical correlations.[1] The most common procedures to determine if sand control is required are described in more detail in the following Sections 2.4.1-2.4.3.

2.4.1 Laboratory experiments

Testing and experimenting on recovered cores from the formation gives useful data of the rocks compressive strength i.e., the hardness of the rock. Since the rocks compressive strength and the drawdown pressure when producing from the reservoir has the same units, the rock strength data can be used to predict the drawdown pressure that will induce the sanding zones in a well. This is a procedure used by most operators. In the early 1970s a research performed at Exxon showed the relationship between the incidence of rock failure and the compressive strength; a rock would fail and begin to produce sand when the drawdown pressure is 1.7 times the compressive strength.[1, 10]

2.4.2 Field observations

Looking at the performance of nearby offset wells is the simplest way of predicting sand production in the field. For an exploration well however, other measures are needed to predict the sanding potential.[1]

To assess the formation stability a sand flow test is often performed. The sand flow test is carried out on surface during a Drill Stem Test (DST) where sand production is detected and measured. Data is collected by gradually increasing the flow rate until one of the following events occur:

- Formation sand is produced
- The capacity of the anticipated flow of the completion is reached
- The maximum drawdown is achieved.[1]

A *sonic log* can be used to evaluate the sanding potential in a well. By recording the required time a sound wave travels through the formation in microseconds the porosity in a certain area can be determined. A 50 microseconds travel time which is a short travel time, is an indication of a hard and dense formation rock with low porosity. Formation rock with higher porosity would have a longer travel time that indicates a softer and less dense formation rock, for instance a travel time

of 95 microseconds. It is a common technique to correlate the sonic logs with incidents of produced sand when determining if sand control is needed or not, this in despite of the fact that it's not entirely reliable.[1, 4]

In addition to sonic logs, density and neutron logs can also indicate the hardness and porosity of a formation; a high-density reading from a density log would indicate a low porosity of the formation, whereas a low-density reading would indicate a high porosity. Neutron logs are primarily used as a tool to indicate formation porosity. The data readings from density, neutron and sonic logs are used together in calculations to determine if the formation will produce sand at certain levels of pressure drawdown.[1, 4]

2.4.3 Theoretical correlations

By correlating the data gathered through field observations and laboratory experiments an accurate prediction of sand production potential can be obtained. In order to achieve this accurate prediction it is necessary to have a detailed knowledge of the mechanical strength of the formation, the in-situ earth stresses and the way the rock will fail.[1]

In a Finite Element Analysis (FEA) model there are developed several geo-mechanical numerical models used to analyze the flow through the reservoir in relation to the formation strength. The effects of the formation stress are associated with the fluid flow within the nearest region around the wellbore, and are therefore simultaneously computed in the FEA. The formation's strength in both elastic and plastic regions where the formation begins to fail is a requirement in a FEA. Under actual downhole conditions it can be difficult to achieve a high degree of accuracy of these regions, which makes the FEA one of the most rigorous and difficult approaches when it comes to predicting the sand production. The FEA is one of the most sophisticated methods to predict the production of sand. [1]

2.5 Sand control methods

Several methods have been developed to prevent and/or reduce the production of formation sand, for instance: restricted and reduced production rate, sand consolidation, gravel packing and resin-coated gravel packing.[11] Depending on the formation properties, one of the following three basic well completion designs is selected for the completion (Fig. 2):

- OH completion
- Cased Hole (CH) completion
- Standalone screen or slotted liner completion

An OH completion can have a perforated reservoir as shown in Fig. 2, or a non-perforated reservoir, this depending on the sand control method to be used and formation properties.

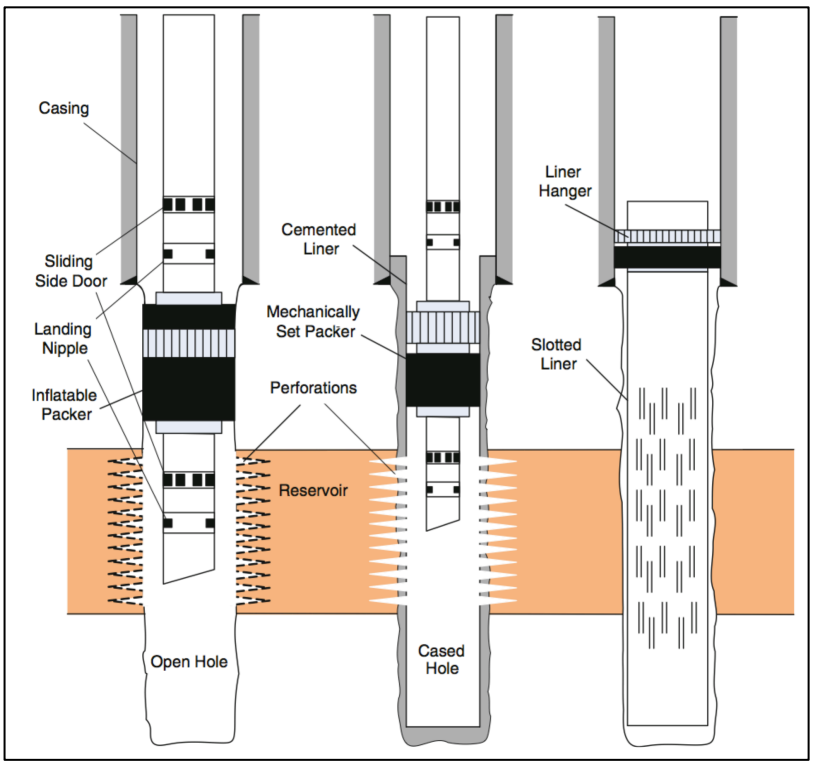

Figure 2: Basic well completion designs: OH, CH and slotted liner completion[5]

2.5.1 Restricted and reduced production rate

Restriction of production rate is the most effective, cheapest and simplest sand control method.[5, 11] By restricting the production rate the sand production can be prevented as the drag forces on the sand grains are reduced. This sand control method does have an important economic aspect since the production rate never can exceed the critical producing rate where sand production becomes excessive.[6, 11] In order to increase the production rates it is possible to use a non-damaging completion fluid together with an increased perforation size and density, this to decrease the fluid velocity and drawdown pressure.[11]

2.5.2 Gravel packing

The mechanical sand control method gravel packing is the simplest, oldest and most consistently reliable method of sand control.[11] Screens are Run In Hole (RIH), and gravel is placed between screen and formation wall. For long producing zones this is the only practical sand control method.[6] The gravel pack methods will be discussed in more detail in Ch. 3.

2.5.3 Resin-coated gravel packing

In a resin-coated gravel pack the gravel is coated with resin and placed both inside and outside the perforations and in the casing. All the sand particles are coated with a very thin layer of resin and are bound together as the resin cures, which result in a highly permeable, strong and synthetic

sandstone filter. In order to have a full-open wellbore the excess resin-coated gravel is drilled from the casing after curing. Resin-coated gravel packing can be used with and without screen, through coiled tubing or concentric tubing, and in remedial or primary work.[11]

2.5.4 Sand consolidation

In plastic treatments resins are injected into the producing interval, binding the formation grains together, this without sealing the pore spaces and therefore maintain the formation permeability. In order to provide the necessary strength to allow high production rates diverting agents and special preflush systems are used to successfully consolidate intervals up to 10 meters.[11]

2.5.5 Standalone screens

Standalone sand screens are installed in the OH section without gravel pack sand between screen and formation wall (annulus). Without the gravel pack placement it is therefore important for both standalone screens and slotted liners that the slot width is of adequate dimension according to the formation sand grains in order to prevent the production of formation sand. Several screens can be used as a standalone screen; wire wrapped screens, expandable screens, pre-packed screens etc. Compared to an ordinary CH completion (with or without production tubing string) the standalone screens are a low cost alternative. Some of the most conventional screens used for sand exclusion can be seen in Fig. 3.[5]

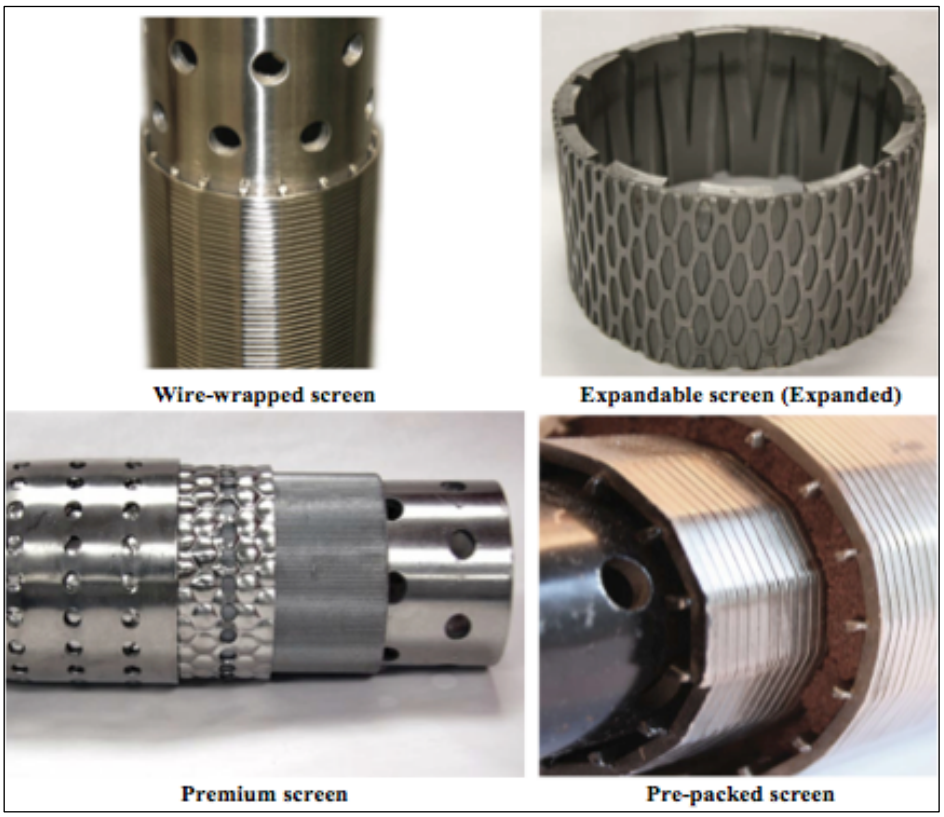

Figure 3: Various screens used in sand control[12]

3. GRAVEL PACKING

3.1 Introduction

Gravel packing is an industry dominant sand control method used to prevent production of formation sand. The gravel pack creates a downhole filter in the wellbore as the properly sized gravel pack sand keeps the formation sand in place, and a properly sized screen or liner keeps the gravel pack sand in place. This downhole filter prevents formation sand from entering the well, but allows formation fluid flow through. As illustrated in Fig. 4, gravel pack operations can be performed in either OH with screens, or in CH where the casing is perforated. The most common method to gravel pack worldwide is with a perforated casing, this due to fewer complications during drilling and completion operations. In Norway however, an OHGP with screens is primarily chosen as the reservoir conditions in most cases are ideal for this.[13]

When vertical and horizontal wells get longer and more complex the operators will often tend to install blank sections of pipe between the screens. As mention earlier this is mainly done in order to achieve zonal isolation between the producing zones, but also due to economical reasons since the blank pipes are less expensive than the screens. The length of a blank pipe section can in some cases be more than 600 meters.[14]

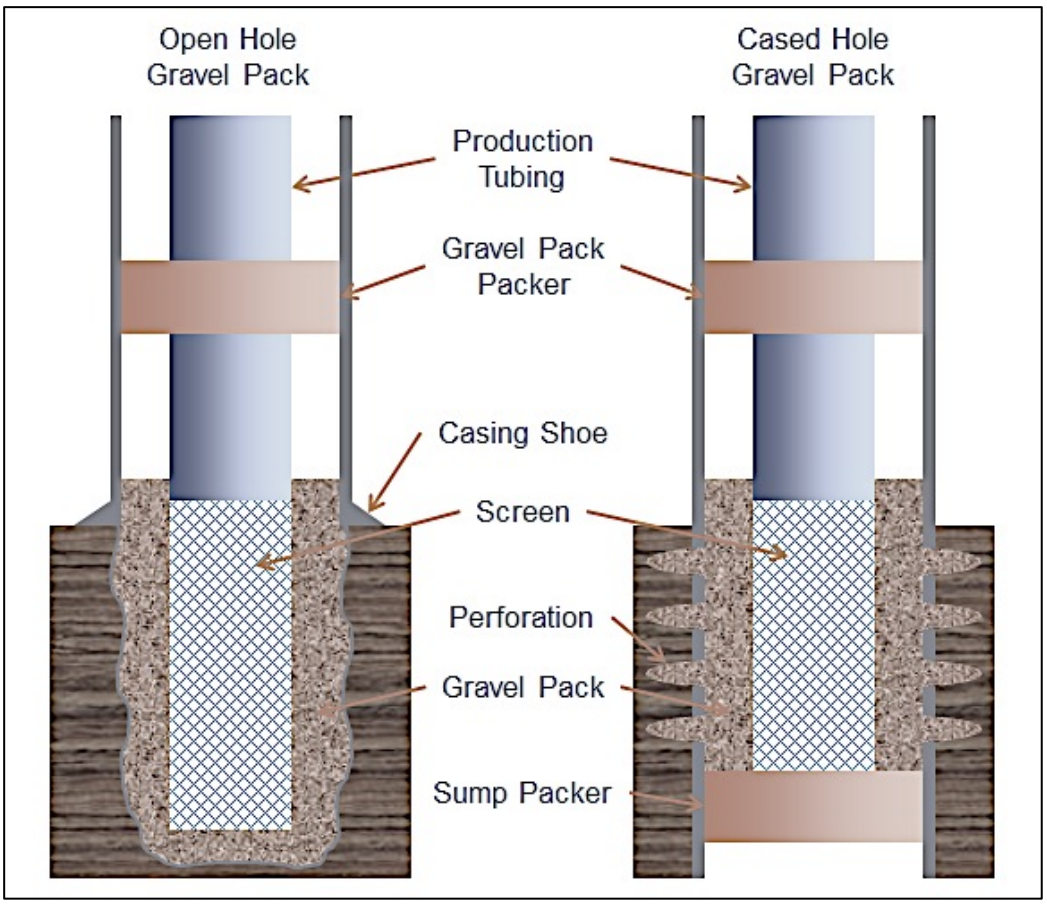

Figure 4: Gravel pack in OH and CH[15]

3.2 Gravel properties and design

With an effective placement technique in addition to an optimized size of gravel and screen slot for the specific formation it is possible to control the formation sand without an excessive reduction in well productivity.

3.2.1 Gravel sizing

The importance of having a truly representative sample of the formation sand, preferably from a full-diameter core is crucial when it comes to the determination of gravel size. With an improper sample of the formation sand the following items can not be determined:[4, 6]

- The proper size of slot, screen or gravel
- The hazards or benefits of acidizing
- The required type and degree of clay stabilization
- The required fluid filtration to avoid damaging the formation

In order to determine the correct gravel size required for a specific job it is necessary to evaluate the Particle Size Distribution (PSD) and the median grain size diameter of the formation sand.[4, 8] A truly representative sample of the formation sand is therefore collected and then tested in a sieve analysis and/or in a Laser Particle Size (LPS) analysis.[5, 12]

In a sieve analysis a dry formation sample is run through a series of woven wire sieves with different mesh size openings in a mechanical sieve shaker. A mechanical sieve shaker can be seen in Fig. 5.

Figure 5: Sieve shaker[16]

The mesh size of a screen is defined by the amount of openings per inch of the screen, which means that with a 100 mesh screen there are 100 openings per inch of the screen. As the mesh size increase will the particle sizes that can pass through the screen decrease. Since different screens can be made out of different thicknesses of wire it makes the mesh sizing an inaccurate measurement of particle size; the thinner the wire get, the smaller the particles passing through the screen, and vice versa. In the mechanical sieve shaker the sieve with the smallest mesh size is placed on top, and the one with the largest mesh size is placed at the bottom.[8, 17] The sieves are typically stacked in 18 steps and have a size range between 2,350 μm and 44 μm.[8] The standard sieve openings for the different United States (US) mesh sizes can be seen in Table 1.

US Mesh	Sieve Opening (in)	Sieve opening (mm)	US Mesh	Sieve Opening (in)	Sieve opening (mm)
2.5	0.3150	8.000	35	0.0197	0.500
3	0.2650	6.730	40	0.0165	0.420
3.5	0.2230	5.660	45	0.0138	0.351
4	0.1870	4.760	50	0.0117	0.297
5	0.1570	4.000	60	0.0098	0.250
6	0.1320	3.360	70	0.0083	0.210
7	0.1110	2.830	80	0.0070	0.177
8	0.0937	2.380	100	0.0059	0.149
10	0.0787	2.000	120	0.0049	0.124
12	0.0661	1.680	140	0.0041	0.104
14	0.0555	1.410	170	0.0035	0.088
16	0.0469	1.190	200	0.0029	0.074
18	0.0394	1.000	230	0.0024	0.062
20	0.0331	0.840	270	0.0021	0.053
25	0.0280	0.710	325	0.0017	0.044
30	0.0232	0.589	400	0.0015	0.037

Table 1: Standard sieve openings[4]

After the sieve shaker process the amount of sand left in each sieve is plotted as a function of the cumulative weight percentage versus the diameter of the sand grains in a sieve analysis plot, which is shown in Fig. 6.[8]

The LPS analysis is a technique based on scattering of light caused by diffraction. To prevent aggregations the formation sand is placed in water with a dispersant, and with a photosensitive detector and a laser the LPS can detect particle sizes down to 0.1 μm. The LPS gives a more representative size distribution of the smaller particle sizes and it is also cheaper, quicker, and requires a smaller amount of formation sand when compared to the conventional sieve analysis. The LPS do also by assumptions on refractive index and adsorption on the particles calculate the volume of a particle passing the detector. The volumetric distribution can therefore be found with a LPS analysis, whereas for the sieve analysis, where a long thin grain can pass a small sieve size will give an incorrect volumetric distribution as the mean diameter of the particle is larger than the sieve opening.[12] After the LPS analysis the measured the particle sizes are plotted as a function of the cumulative volume percentage versus the diameter of the sand, shown in Fig. 7.

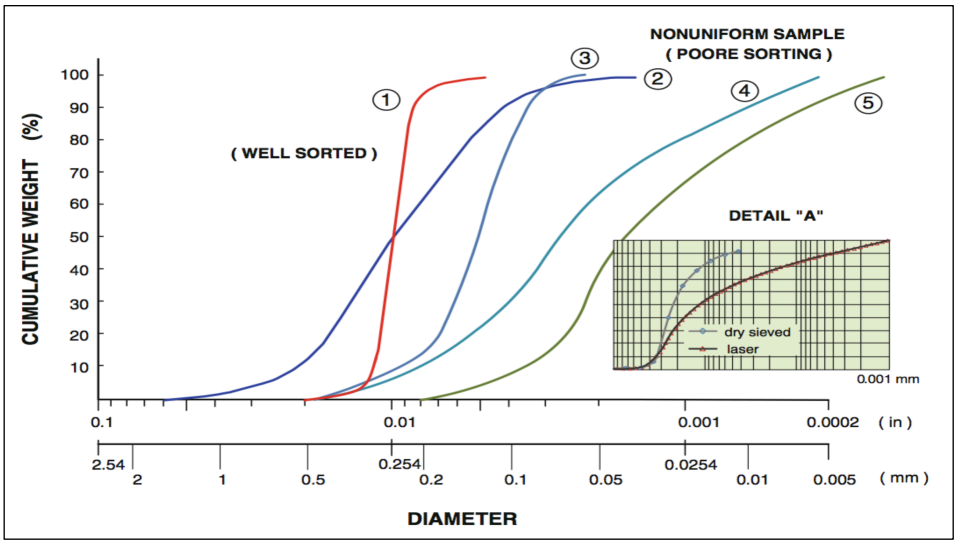

Figure 6: Sieve analysis plot: (1) Uniform sample, (2) non-uniform sample, (3) gas well offshore at 628 m, (4) gas well offshore at 850 m, (5) oil well at 875 m. Detail "A": Difference in curve for LPS and sieve distribution for the same sample[5]

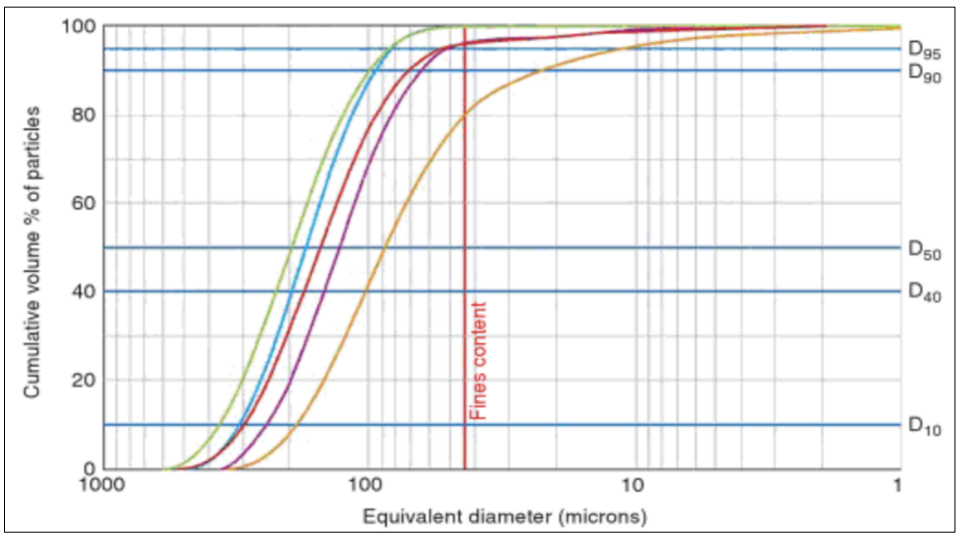

Figure 7: LPS analysis: Cumulative volume percentage versus sand diameter for several depths [12]

From the sieve analysis and LPS plots it is possible to determine if the formation sand is uniform or not. A uniform sample describes particles that are well sorted within a narrow size range, and a non-uniform sample describes poorly sorted particles with a broader size range. An example of a uniform and a non-uniform sample is shown graphical in Fig. 6, where a comparison between the measured diameters of the particles in a sieve analysis and a LPS also is shown.[5]

The uniformity of the formation sand can also be presented as shown in Fig. 8, where the weight percentage versus the particle diameter are plotted. The *median* formation grain size d_{50}, which splits the distribution into two equal parts can be read at the 50% cumulative level and is used together with d_{10}, d_{40} and d_{90} to determine the optimal size of the gravel needed to hold the formation sand in place.[4, 8, 17]

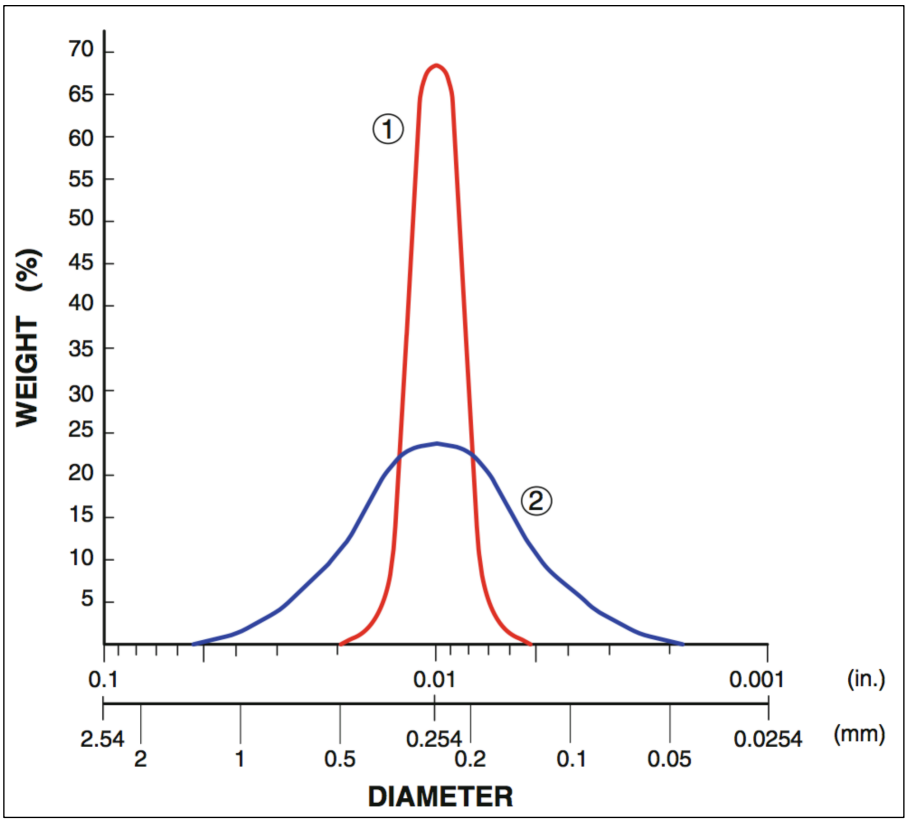

Figure 8: (1) Uniform sample, (2) non-uniform sample determined by weight percentage versus particle diameter[5]

The uniformity coefficient C_u, is expressed as the ratio of the d_{40} and d_{90} shown in Eq. 1, and the sorting coefficient, S_o, is expressed by the squared root ratio of d_{25} and d_{75} shown in Eq. 2. A perfectly uniform sample would have a uniformity and sorting coefficient of 1.0, whilst a non-uniform sample would have a uniformity coefficient higher than 5. An overview of Schwartzs suggested gravel sizes with respect to uniformity can be seen in Table 2, where D_{10} describes the 10 percentile of the gravel diameter.[5]

$$C_u = \frac{d_{40}}{d_{90}} \qquad \text{Equation 1}$$

$$S_o = \sqrt{\frac{d_{25}}{d_{75}}} \qquad \text{Equation 2}$$

Diameter percentile of:				
Gravel		Formation sand	Uniformity	Distribution uniformity
			Perfect uniform sample	$1 = C_u = S_o$
D_{10}	=	$6d_{10}$	For uniform sands	$C_u < 3$
D_{40}	=	$6d_{40}$	For non-uniform sands	$5 < C_u < 10$
D_{70}	=	$6d_{70}$	For extremely non-uniform sands	$10 < C_u$

Table 2: Suggested gravel sizes based on the uniformity of the formation sand[5]

3.2.2 Gravel-sand size ratio

The optimal Gravel-Sand (G-S) ratio has not been standardized, but was early investigated by Coberly, Hill, Wagner and Gumpertz who meant that the G-S ration was equal to the largest gravel size divided by the 10 percentile of the sand size. The more known G-S ratios from Maly, Schwartz and Sauciers are shown respectively in Eqs. 3-6 (Two equations for Maly).[6]

$$\text{G-S ratio} = \frac{\text{smallest gravel size}}{\text{10 percentile sand size}} \qquad \text{Equation 3}$$

$$\text{G-S ratio} = \frac{\text{10 percentile gravel}}{\text{10 percentile sand}} \qquad \text{Equation 4}$$

Or

$$\text{G-S ratio} = \frac{\text{40 percentile gravel}}{\text{40 percentile sand}} \qquad \text{Equation 5}$$

$$\text{G-S ratio} = \frac{\text{50 percentile gravel}}{\text{50 percentile sand}} \qquad \text{Equation 6}$$

Laboratory work by Saucier shows the best effect of G-S ratio on gravel pack permeability, where the ideal G-S ratio is in the range of 5-6. The median of the grain size of the gravel should therefore be up to six times larger than the median of the grain size of the formation sand found in the PSD analysis: $D_{50} = 5\text{-}6d_{50}$.[5, 6] Saucier's experimental work results for an optimized gravel size and the recommended guidelines for gravel sizes (based on Saucier's work) can be seen in Fig. 9 and Table 3.

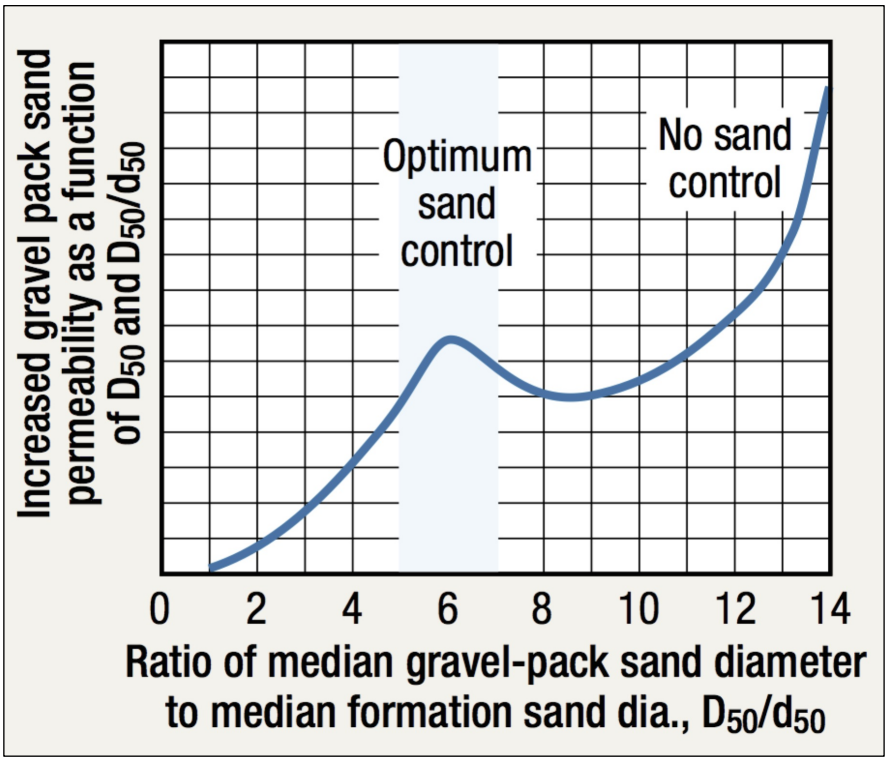

Figure 9: Saucer's results for an optimized gravel size[4]

	d_{50}/d_{50}	<	5	Good sand control, but low gravel permeability restricts the flow
5 <	d_{50}/d_{50}	<	7	Good sand control; maximum pack permeability
7 <	d_{50}/d_{50}	<	9	Good sand control, but formation sand invasion of gravel pack restricts the flow
9 <	d_{50}/d_{50}			No sand control; formation sand travels through gravel pack

Table 3: Guidelines for an optimal gravel size[4]

The formation sand is analyzed and the correct gravel size is chosen for the specific job. The gravel sand size is categorized and named after the mesh size. A 20/40 mesh gravel describes gravel sizes between 40 and 20 mesh, where 40 mesh is the smallest gravel size.

3.2.3 Gravel type and quality

Besides the determination of the optimal gravel size for a specific job it is of importance that the gravel is of high quality. The quality of gravel is among others measured by roundness, sphericity, grain multicrystallinity, and permeability. The American Petroleum Institute (API) Recommended Practices (RP) 58; *Testing Sand Used In Gravel Packing Operation* proposes the specifications for high quality gravel. A crush-resistance test is one of the methods proposed by API where the amount of fines generated is measured. Since the presence of fines in a gravel pack will reduce the permeability API proposes as a basic requirement a minimum of fines generated during a crush test. Some of the specifications from API RP 58 can be seen in Table 4.[18-20]

Grain Size (US mesh)	8/16	12/20	16/30	20/40	30/50	40/60
Nest of sieves recommended for testing	6	8	12	16	20	30
	8	12	16	20	30	40
	10	14	18	25	35	45
	12	16	20	30	40	50
	14	18	25	35	45	60
	16	20	30	40	50	70
Property	Specification					
Sieving	A minimum of 96% should pass the coarse designated sieve. A maximum of 1/10% should be larger the largest sieve size. A maximum of 2 % should be smaller than the smallest sieve.					
Sphericity	≥ 0.6					
Roundness	≥ 0.6					
Crush resistance	8/16	12/20	16/30	20/40	30/50	40/60
Stress on sand	2000 psi					
Maximum fines by weight	8%	4%	2%			

Table 4: API specifications for high quality gravel grain[19]

Gravel pack sand can be divided into two different categories:

- Natural gravel
- Synthetic gravel

The natural gravel is predominated to almost exclusive applications due to the unlimited availability and the low cost, but the quality varies enormously in terms of roundness and sphericity.[12, 21] The so-called man-made or synthetic gravel is of ceramic material, and because of the improved roundness and the greater strength the permeability is higher compared to naturally occurring gravel. This high permeability and strength gives several advantages as increased crush resistance and a slightly better tolerance to fines invasion.[12] Fig. 10 show synthetic gravel pack sand in different US mesh sizes.

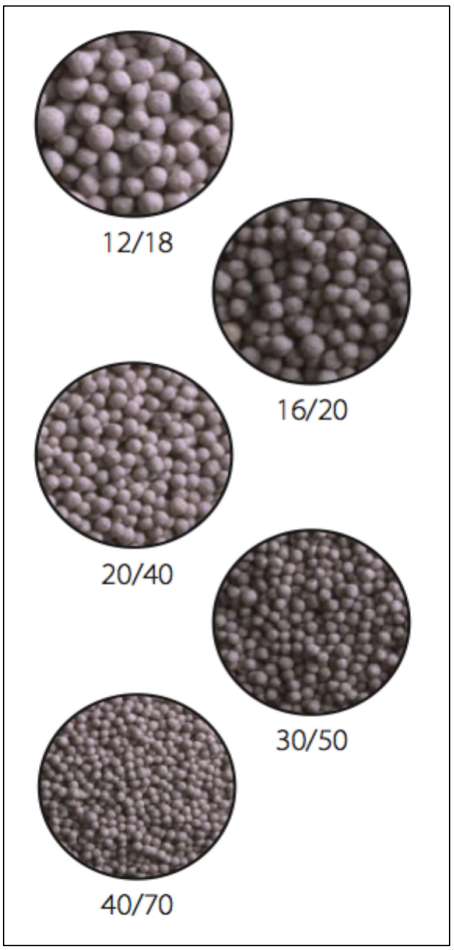

Figure 10: Synthetic gravel in several US mesh sizes[22]

3.3 Screen sizing

When determining the screen size it is desirable to have a slot width as large as possible in order to minimize the restriction of fluid flow and interstitial fines, but at the same time a small enough width to retain the sand grains. According to Coberlys experimentally work should there be an upper limit for the slot width of no more than twice the 10 percentile from the PSD analysis.[6, 23] With a larger slot width, an effectively bridging would be difficult to achieve. To retain gravel, the screen size should generally be no larger than the smallest gravel size, usually 2/3 to 1/2 of the smallest gravel.[6]

The slot width or wire spacing is measured in thousandths of an inch, also called gauge. A 20 gauge screen would therefore have a screen opening of 0.020 in. Table 5 shows an overview of the most common choices of screen openings determined by the gravel size.

Gravel size (U.S. Mesh)	**Gravel size** (in.)	**Screen opening** (in.)	**Screen opening** (gauge)
40/60	0.0165-0.0098	0.008	8
30/50	0.0230-0.0120	0.010	10
20/40	0.0330-0.0165	0.012	12
16/30	0.0470-0.0230	0.016	16
12/20	0.0660-0.0330	0.020	20
8/12	0.0940-0.0470	0.028	28

Table 5: Screen opening for various gravel sizes.[4]

3.4 Carrier fluids

The main objective with carrier fluids used in gravel pack operations is to carry the gravel efficiently into and out of the wellbore.

Brine, as the simplest carrier fluid was before the early 1960s the most common fluid in use for transporting gravel in gravel pack operations. This was mainly due to the lack of development of other fluid systems. Since then there have been used several types of carrier fluids to transport gravel into or out of the wellbore. This includes among others brine, diesel, oil, foam, cross-linked gels, Clarified Xanthum (XC) gum gel, and Hydroxy-Ethylcelluse (HEC) gel. The most common carrier fluids in use today are brine and HEC gel, where brine is the most common carrier fluid used in Norway.[4, 24]

Carrier fluids can mainly be divided into two groups: Water or conventional packs, and viscous or slurry packs. In a viscous pack it is the viscous forces that mainly influence the gravel, whereas in a water pack it is the gravity forces that mainly influence the gravel.[4] Water packs are normally preferred over slurry packs since the polymer residue from viscous packs can damage formation permeability. The water packs can contribute to form a tight annular pack, but have the disadvantage of a high leak-off rate in high permeable zones compared to a viscous pack. This high leak off can result in a bridging of the screen, and with a restricted fluid flow to the screen will cause in a rapid increase in pump pressure causing an early screenout.[4]

HEC gel is the most preferred viscous pack due to its low cost and the wide availability. A disadvantage with HEC is the formation of “fish-eyes” that comes through an ineffective dispersion of HEC powder in brine. A liquid HEC has been introduced in order to avoid the formation of “fish eyes”.[25] The most common water pack carrier fluid used is brine due to its low cost and wide range of densities with regards to pressure control.[25] The density of the brine is determined by reservoir pressure, formation stability, risk of cave in and fluid loss to formation. In Table 6 the most common water based gravel pack fluids are listed with their respective Specific Gravity (SG) when saturated.[8]

Brine	Molecular formula	SG (Saturated)
Sodium Chloride	NaCl	1.20
Sodium Bromide	$NaBr_2$	1.53
Calcium Chloride	$CaCl_2$	1.39
Calcium Bromide	$CaBr_2$	1.86

Table 6: Most common water based gravel pack fluids [8]

The difference in viscosity, typical pump rate and gravel concentration for brine water pack and HEC gel viscous pack can be seen in Table 7.

	Brine		HEC gel	
Viscosity	1-2	cp	300-750	cp
Typical gravel concentration	1-3	ppg	10-15	ppg
Typical pump rate	4-5	bpm	1-4	bpm

Table 7: Comparison of brine water pack and HEC gel viscous pack[4]

The choice of carrier fluid for a particular application is determined by several factors like completion type, well inclination, temperature, interval length, formation permeability, reservoir fluid, cost and pressure to mention some. Laboratory testing, nodal analysis, reservoir simulation and gravel placement simulations are normally carried out when selecting the carrier fluid.[25]

3.5 Vertical openhole gravel packing procedure

When the reservoir section of a vertical well has been drilled, the drilling fluid is displaced with a solids-free or low solids water-based completion fluid (Brine) in the openhole.[12] The gravel pack packer and the screen with Washpipe (WP) inside are RIH together, and the gravel pack packer is then set just above the lowest casing shoe as illustrated in Fig. 11. In the lower end of the screen a bull nose is placed for both guidance down the well and for prevention of the gravel to pack inside the screen. Both WP and screen is connected to the crossover tool, which is placed right above casing shoe.

A Constant Level Additive Mixer (CLAM) makes sure that the desired concentration of gravel and brine is mixed together. The slurry is then injected down the drillpipe with a pumping rate of approximately 1,000 litres per minute via the pump. The slurry flows down the drillpipe to the crossover tool, where it continues through the crossover ports and enters the annulus between casing and screen just below the packers. The slurry continues to flow down the annulus between the formation wall and the wire-wrapped screen until the gravel due to gravity falls out of suspension and then starts to pack. The gravel will fall out of suspension and the brine flow will split into two separate flows; one flow in the annulus between the formation wall and the screen, and another one in the mini-annulus between the screen and the WP. As the gravel packs around the screen the brine will leak off through the screen from annulus and flow down the mini-annulus between screen and WP and eventually be carried back to surface through the WP and crossover tool. The brine is crossing back to the annulus right above the packer. When the whole screen is covered with gravel it will cause a sudden and significant restriction to fluid flow since

the brine now cannot enter the screen and therefore has nowhere to flow. The restricted fluid flow results in a rapid increase in pump pressure defined as a screenout. The screenout can easily be seen on the pressure graphs on the logging computer on the rig. To avoid the formation from fracturing it is necessary for the pump to be switched of as quickly as possible when the screenout occurs.

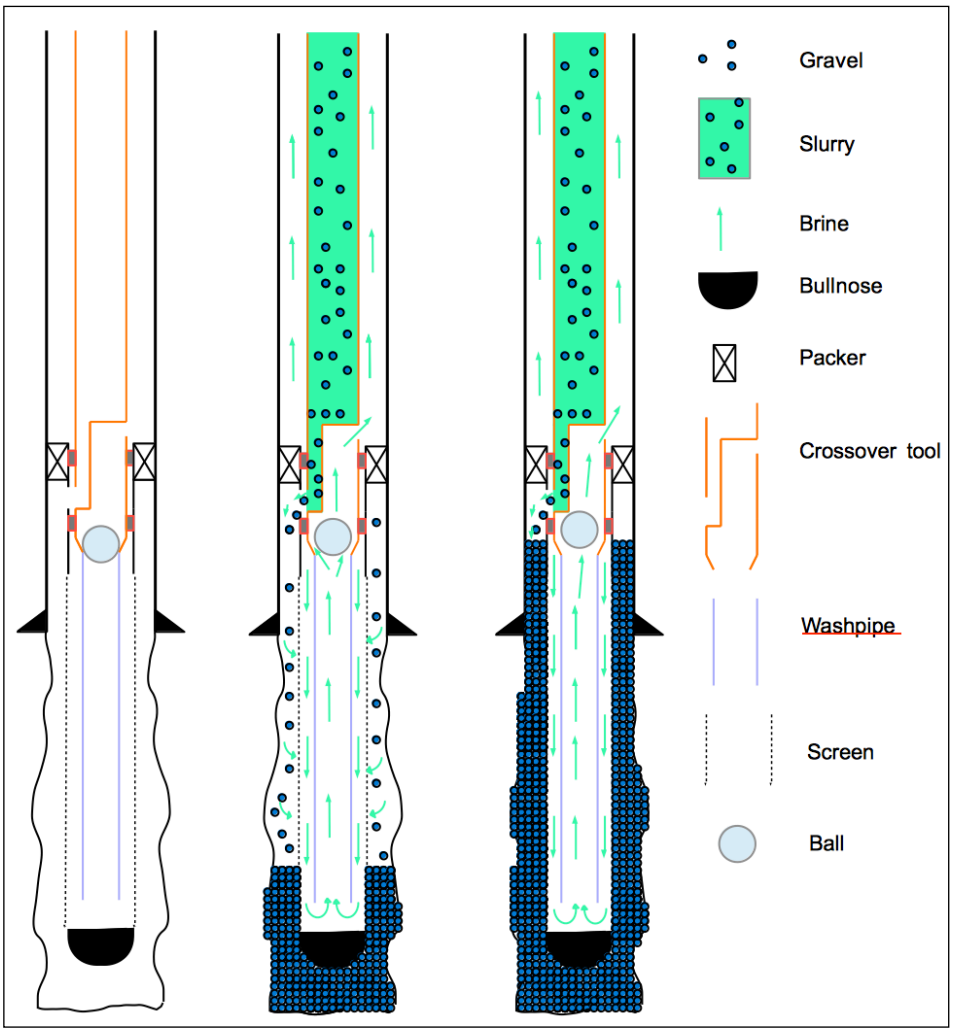

Figure 11: Vertical gravel packing in OH

When the pump is shut off, the drillpipe is still filled with slurry that needs to be transported to the surface before the gravel settles out. If gravel do settle out in the drillpipe the sand control service string may get stuck, which again can result in shutting down the well. Right after screenout when the pump has been shut off it is therefore important to pull the service tool up so the lower crossover ports are placed above the gravel pack packers in a reversed circulation position (See Fig. 12). In the reversed circulation position a completion brine is pumped down annulus with a high enough rate to lift the excess gravel in the drillpipe. The brine flows down annulus from surface, through the lower crossover port and then forces the slurry up the drillpipe and up to surface. The gravel pack operation is now finished.

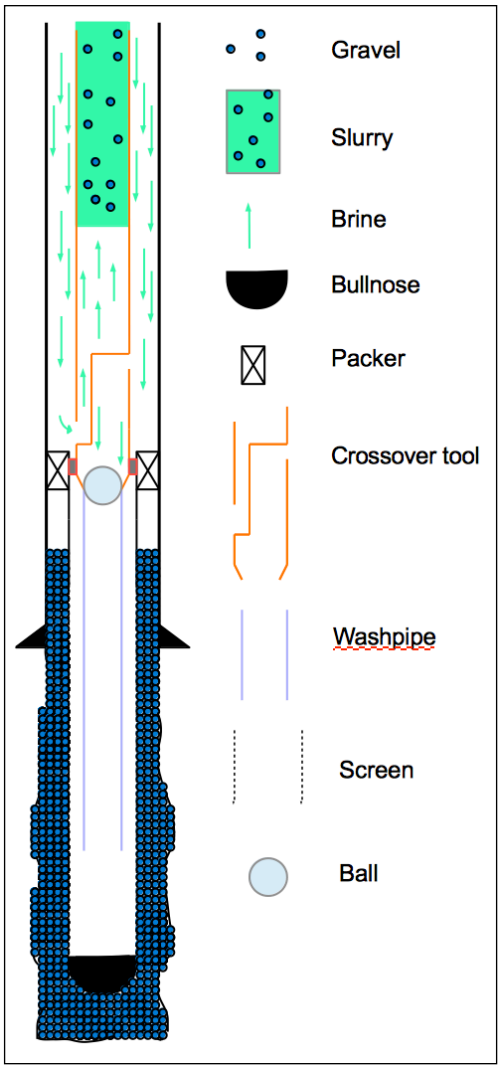

Figure 12: Reversed flow

3.6 Vertical gravel packing in openhole with blank sections

In a conventional vertical OHGP operation as described in Section 3.5 the whole screen length will eventually be packed with gravel. In a vertical OHGP blank sections of pipe can be placed between the screen sections in order to seal of zones and/or to reduce the costs as mentioned earlier. With a blank pipe section installed it results in a different gravel placement and settling behaviour compared to a conventional OHGP operation. In the lower section of the well the gravel will pack around the lower screen section as in a conventional OHGP operation, but as soon as the gravel has packed around this screen and the brine can no longer access through it due to the packed gravel the settling regime changes. With the overlying section being of blank pipe is it necessary for the brine to flow upwards to the upper screen in order to make room for the gravel to pack in the blank pipe section. Therefore, when the lower screen section is packed and the blank section is filled with slurry the gravel will displace the brine mainly due to gravitational forces. Fig. 13 illustrates the gravel pack process for a vertical OHGP with blank pipe sections.

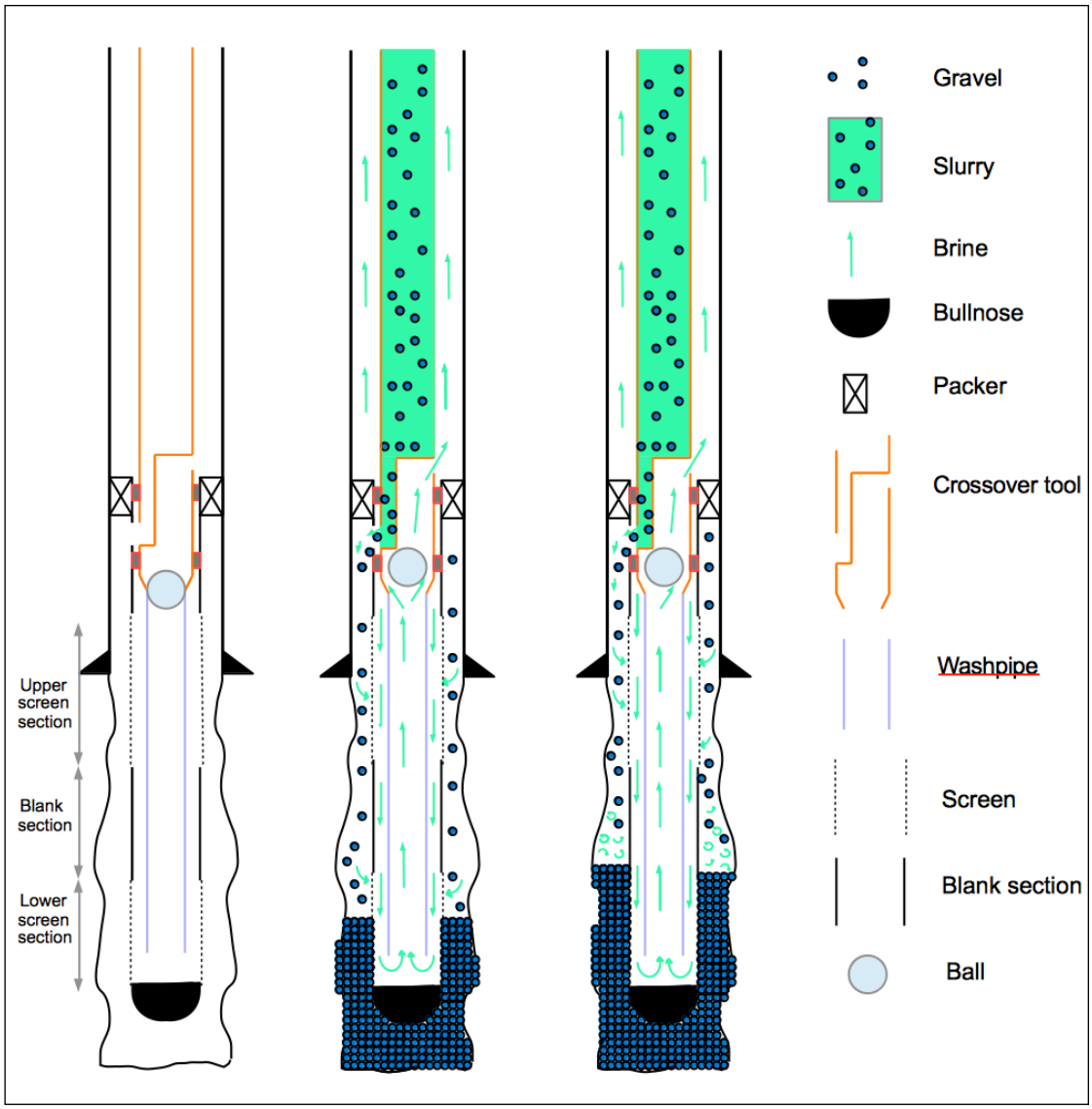

Figure 13: Vertical gravel packing in OH with blank sections

3.7 Gravel settling in blank section

In order to do a cost effective and good gravel pack job in a well with blank sections it is important to understand the different settling models that apply.

3.7.1 Vertical gravel settling regime

For a gravel to settle in a vertical OHGP it is necessary for the gravel to switch place with the carrier fluid that is already placed in the well. When a certain volume of gravel settles in a blank section the same volume of carrier fluid will be pushed upwards. The forces that act on the gravel in a fluid in a vertical section is described in more detail in Ch. 5.

3.7.2 Inclined gravel settling regime: Boycott

In an inclined well with blank sections however, the gravel will settle differently compared to a vertical well. The gravel settlement regime changes as the gravel tend to “slide” on the lower side of the well. This “sliding” of gravel is called the Boycott settling effect after the physician Acrivos Boycott. It was in the 1920’s when Boycott found out that inclined tubes will cause an increase in the settling rate since the sedimentation path is shorter compared to vertical tubes. Due to density differences and inclination the rising liquid and the falling particles will get out of each others way easier, this causing an accelerated settling.[26-28] Studies on cement plugs placement and barite sag in deviated wellbores have concluded that the boycott effect increases when the density differential between the separated fluids/particles increases.[29, 30] This increased boycott effect will also apply for gavel settling when the density difference between carrier fluid and gravel is increased. An illustration of the Boycott settling effect can be seen in Fig. 14.

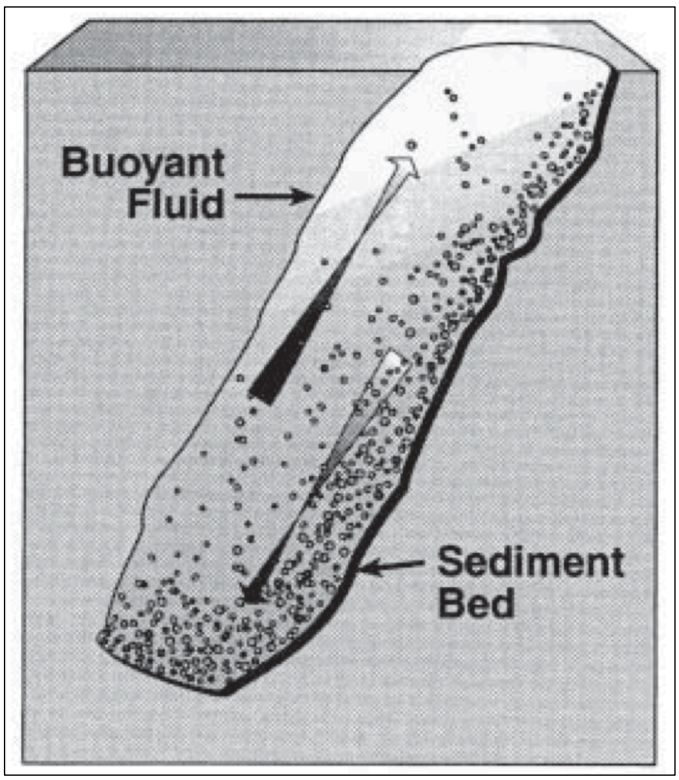

Figure 14: Illustration of the Boycott settling effect[31]

4. CASE MODEL

In order to make the calculations as realistic as possible is the case model used for calculations in this thesis based on an actual well in the Norwegian sector. The original well trajectory of the well has been straighten out and then the lower completion has been placed in a 30 degree angle from the vertical, this to simplify the calculations. Shortening the Measured Depth (MD) of the modified well trajectory will make the True Vertical Depth (TVD) consistence with the original well. This makes it possible to use the original temperature- and pressure data from the original well for the modified well. A sketch of the modified well used in this thesis can be seen in Fig. 15.

Looking at how the gravel packs and settles in the lower screen section and the blank pipe section separately will simplify the calculations. The scenarios to be calculated are described in more detail in the following Sections 4.1 and 4.2.

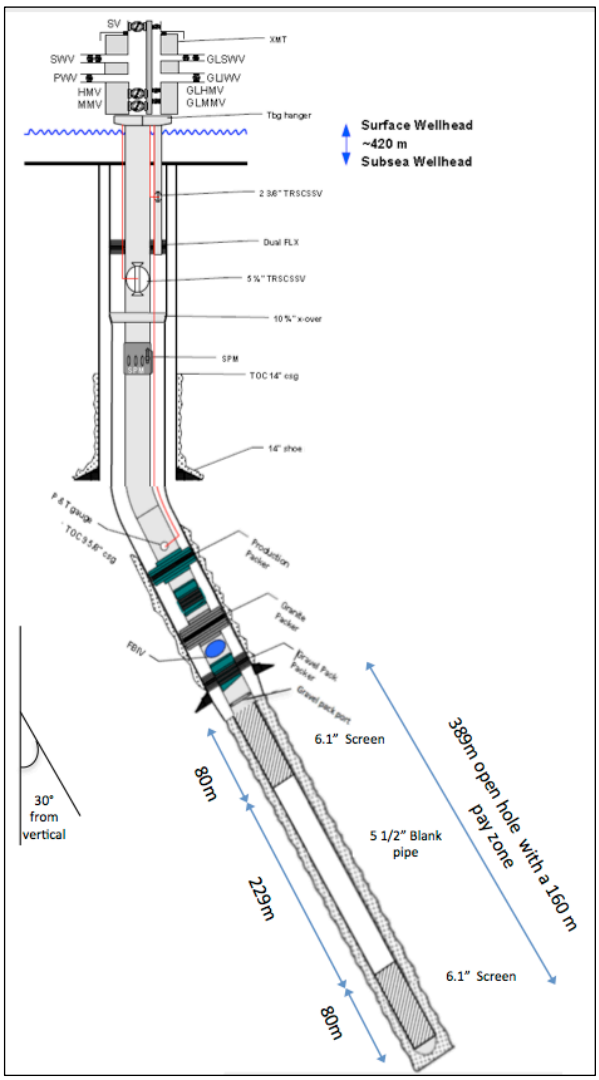

Figure 15: Illustration of the modified well

4.1 Scenario 1: Gravel packing lower screen section

The gravel placement in the lower screen section settles as in a conventional OHGP. The slurry is pumped down the annulus and a split flow occurs in the upper and lower screen section. A percentage of the carrier fluid flows through the screen and down mini-annulus. After the flow split in the upper screen section the density of slurry that continues down annulus will increase. Calculations on gravel packing in the lower screen section are carried out in Ch. 6.

4.2 Scenario 2: Gravel packing in blank section

The gravel settling and placement in the blank pipe section is mainly affected by gravitational forces and the boycott effect described in Section 3.7. With the assumption of no flow of carrier fluid through the gravel pack around the lower screen this section can be looked at as an inclined tube with a closed end.

A certain concentration of gravel is pumped down the annulus continuously together with the carrier fluid. In order for the gravel to settle in the blank pipe section the same volume of carrier fluid must be displaced from the same area. This volume of brine will flow upwards to the upper screen section and continue down mini-annulus, through the WP and up to surface. To obtain a good gravel pack in the blank pipe section it is necessary for the gravel to have a certain settling velocity to avoid accumulation of gravel near the upper screen section. Accumulation of gravel near the upper screen section due to low gravel settling velocity in the blank pipe section can lead to a packed upper screen and an unpacked blank section. With this scenario, the gravel from the upper screen section will over time settle due to gravitational forces, leaving the upper screen section unpacked. In theory this means that the gravel to be packed in the blank pipe section need a minimum settling rate equal to the rate of gravel that is pumped down the well from surface. Calculations on gravel packing the blank pipe section are carried out in Ch. 6.

4.3 Assumptions for case model

Due to time limitations on this thesis and the fact that calculations are to be made on a modified field case a number of assumptions are needed in order to describe the different phenomena. These assumptions simplify the calculations and are described in more detail in the following Sections 4.4.1-4.4.8

4.3.1 No rat hole or underreamed hole

The rat hole is an extra hole drilled below the pay zone and is used to drop of expendable completion equipment or to gather liquid that is to be separated from gas prior to being pumped out of the well. To simplify the calculations with regards to pressure and gravel settling it is assumed that the case model does not have a rat hole.[32, 33]

An underreamed hole (Fig. 16) is an enlargement of the already drilled OH and is normally carried out in order to remove damage that is present in the initial OH, or to provide greater clearance between the screen and the formation wall. This thesis assumes no underreamed OH.

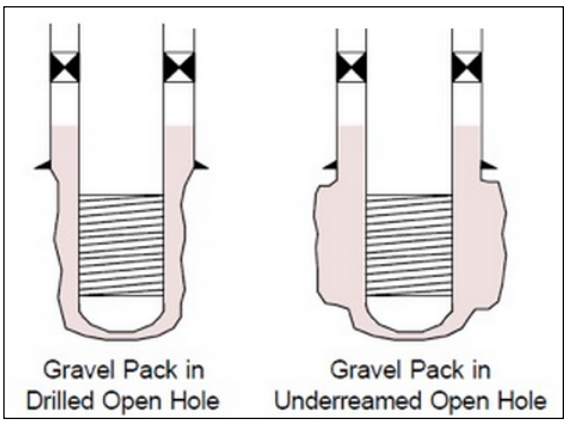

Figure 16: Sketch of underreamed OH[34]

4.3.2 A concentric configuration in well

From Fig. 17 the different annuli configurations for a well can be seen. The eccentricity *e,* describes how off-centered a pipe is within another pipe or OH. In a horizontal well a pipe in the OH would be fully eccentric with an eccentricity of 1, whereas for a vertical well the pipe in the OH would be concentric with an eccentricity equal to zero. An inclined well will be partially eccentric. In order to avoid problems related to eccentricity it is common to use centralizers to obtain a concentric well. In this thesis it is assumed to have a concentric configuration in the well for both vertical and inclined sections. This applies for all pipes and OH.

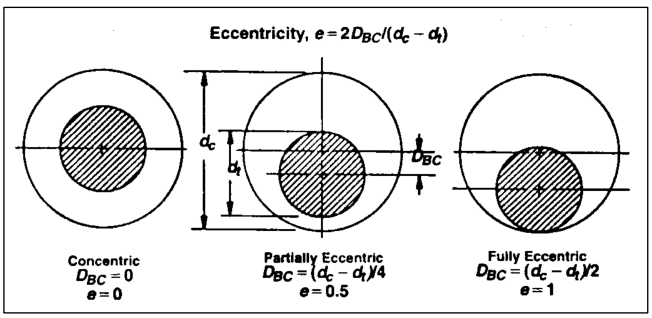

Figure 17: Annuli configurations[35]

4.3.3 Gravel properties and behaviour

The settling velocity for a given particle is among other dependent on shape and size. The gravel grains in this thesis are assumed to be fully spherical, fully round and perfectly uniform in distribution. When calculating the settling velocity of the gravel, the mechanisms that include particle interaction are not taken into account as this complicates the settling equations drastically.

4.3.4 No fluid loss to formation

The loss of fluid to the formation during gravel pack operations is normally unavoidable and can some times be severe. With an impermeable filter cake from the drilling fluid it is possible to either reduce, or completely avoid any fluid loss to the formation. In this thesis it is assumed that the impermeable filter cake prevents any fluid loss to the formation and the returning fluids will therefore have a rate equal to the pumping rate.

4.3.5 No fluid flow through packed gravel

The flow of fluid through a porous medium, known as Darcy's law is valid for any Newtonian fluid and can be seen in Eq. 7.

$$Q = -K\frac{A}{L}\Delta h \qquad \text{Equation 7}$$

Darcy's law states that the fluid flow rate through a porous media is proportional to the head loss and is inversely proportional to the length of the flow path. A one-dimentional flow column through a porous medium can be seen in Fig. 18.[36]

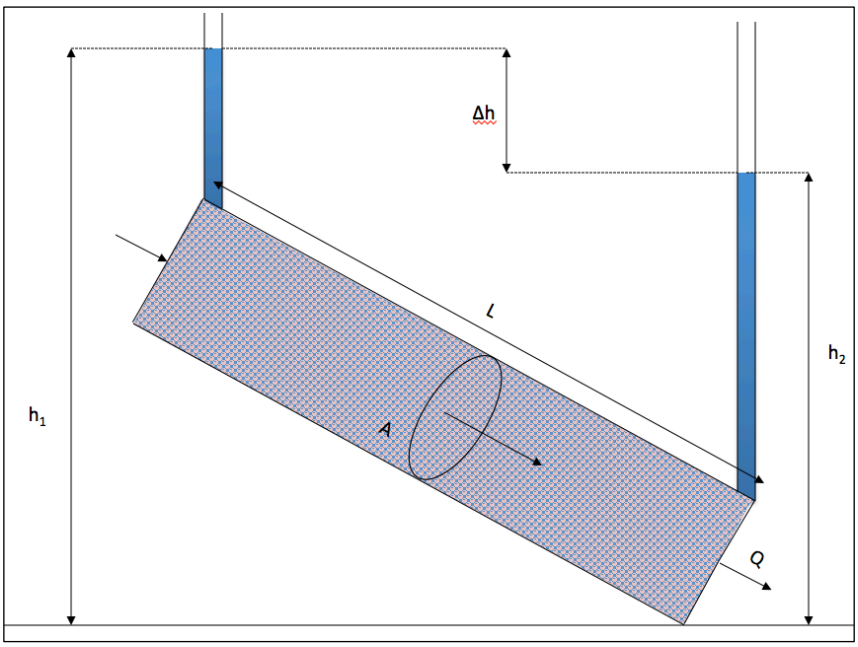

Figure 18: One dimensional flow column through a porous medium

The packed gravel has a permeability that allows carrier fluid to flow through. A flow of carrier fluid through this packed gravel effects the pressure drop, and therefore also affects the flow split in the screens sections. By assuming no fluid flow through the packed gravel, the settling velocity term for free falling particle can be carried out in the blank pipe section. Due to inclination it is assumed that the lower screen section is completely packed before gravel starts to pack in the blank pipe section.

4.3.6 Newtonian carrier fluid

A Newtonian carrier fluid with low viscosity is used for calculation in this thesis. A Newtonian fluid exhibits a linear relationship between shear strain and shear stress, and will therefore have the same viscosity weather it is exposed to high or low shear. The difference between Newtonian and non-Newtonian fluids with regards to shear rate and shear stress can be seen in Fig. 19.

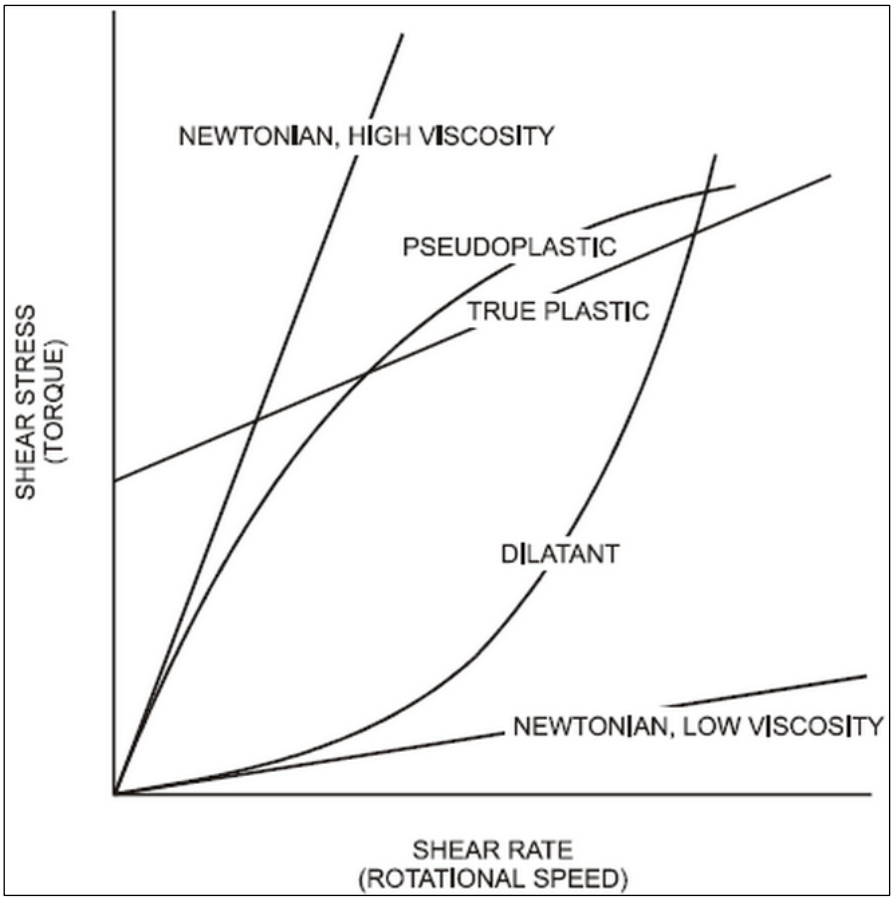

Figure 19: Behavior of Newtonian and Non-Newtonian fluids[37]

4.3.7 No pressure drop between annulus and mini-annulus

When the flow splits between annulus and mini-annulus as described in Section 3.5, the flow will be balanced since the flow paths are parallel and the resistance between them can be negligible. This gives a pressure gradient balance between the two annuli.

4.3.8 Neglect pressure drop due to acceleration

The acceleration pressure drop can only be significant in cases where the velocity undergoes great changes over a short section of pipe. These conditions can only exist with very high flow velocities and certain flow patterns and is therefore negligible for vertical and slightly inclined wells.[38]

5. SUPPORTING THEORY

In this chapter the supporting theory for the calculations in Ch. 5 is presented. Mathematical models are derived and fundamental theories in physics are described in detail. It is assumed that the reader has a basic knowledge of geometry.

5.1 Geometry of wellbore

5.1.1 Hydraulic diameter

In order to determine whether the flow is either in a laminar or a turbulent flow regime it is necessary to calculate the Reynolds number. The hydraulic diameter, D_H, is used to calculate the Reynolds number and is therefore introduced when handling flow in a noncircular tube or channel. The hydraulic diameter is defined in Eq. 8, where A represent the cross sectional area, and p represent the cross section of the wetted perimeter.[39]

$$D_H = \frac{4\,A}{p} \qquad \text{Equation 8}$$

In a vertical or inclined well with a concentric annulus the hydraulic diameter can be calculated from the known inner and outer diameter of the pipe. This is shown in Eq. 9.

$$D_H = \frac{4\,\pi\,({D_o}^2 - {D_i}^2)}{\pi\,(D_o - D_i)} = D_o - D_i \qquad \text{Equation 9}$$

The OH, screen, WP, and blank pipe, also called Base Pipe (BP) have all different diameters which effects how and where the slurry and carrier fluid flows. Figs. 20 and 21 illustrates the geometry of the cross sectional areas used for calculation of flow downhole during the OHGP in this thesis.

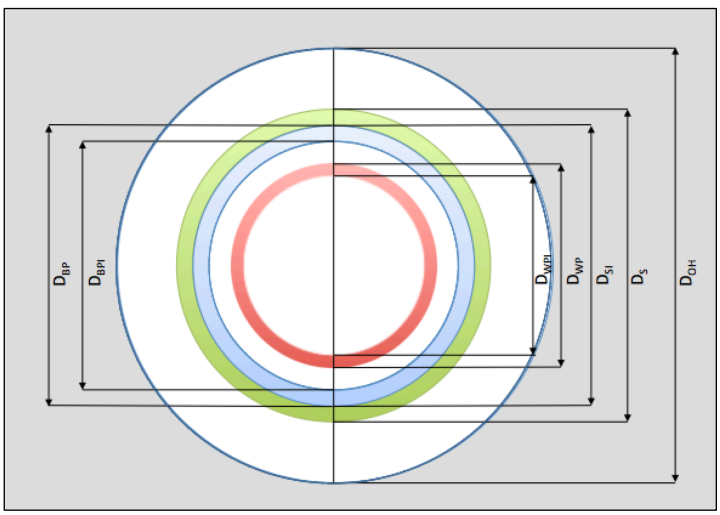

Figure 20: Cross sectional area in screen section

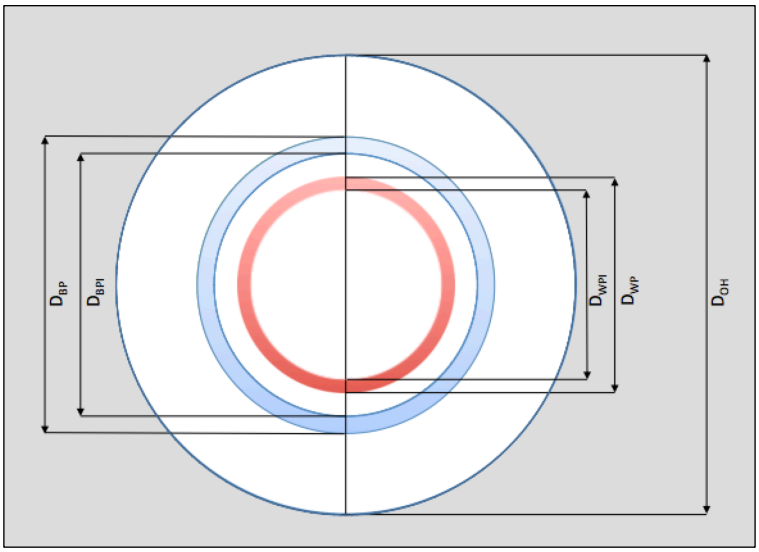

Figure 21: Cross sectional area in blank pipe section

5.2 Gravel settling velocity in blank section

When the lower screen section is packed with gravel and gravel starts to settle in the blank section the brine will move upwards to the upper screen section due to displacement from gravel and because it is the easiest path with regards to pressure. There will in reality be a percentage of brine that flows through the packed gravel and through the lower screen section. The more gravel that packs in the blank section will decrease the percentage of brine passing through due to a lower permeability in the gravel pack. For simplicity with regards to the calculation it is therefore assumed that when the gravel has packed around the lower screen section the brine will not be able to move through the gravel pack. The only option for the brine to flow is then upwards through the upper screen section. See Fig. 22 for carrier fluid flow path used for calculation.

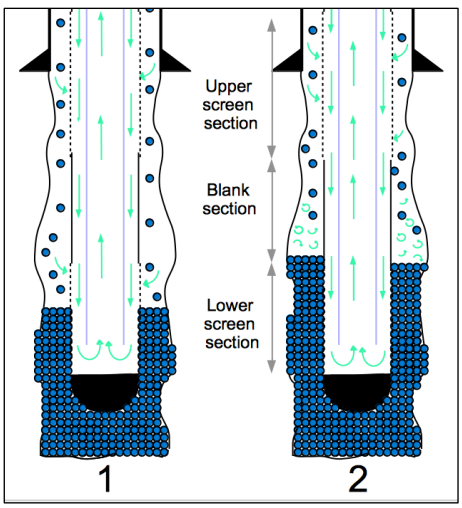

Figure 22: Carrier fluid flow in OHGP with blank sections; (1): Packing lower screen section (2): Packing blank section

5.2.1 Vertical settling velocity

Fig. 23 illustrates the forces that act on a single gravel in a fluid in a vertical section. The gravel have a gravitational force F_g, downwards and a frictional drag force F_d, caused by the brine moving upward as the gravel is taking up more and more space.[26, 40]

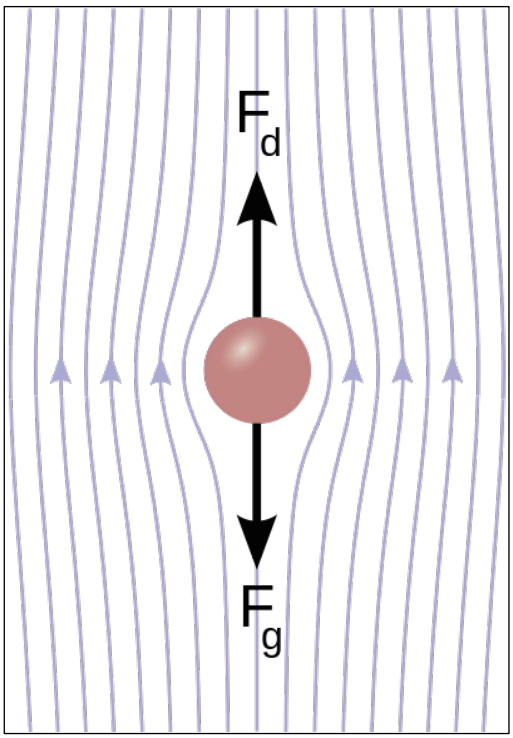

Figure 23: Drag and gravity force on a single particle in fluid[40]

The frictional drag force F_d will increase as the velocity of the particle increases. For spherical particles like gravel the drag force can be calculated as in Eq. 10, where μ is the fluid viscosity, and r_p is the radius of the particle.[26]

$$F_d = 6\pi\mu r_p{}^2 \qquad \text{Equation 10}$$

The gravitational force Fg, can be derived from Newton's second law shown in Eq. 11, where v_s is the settling velocity of the particle with a mass m at time t.

$$F_d - F_g = m\frac{dv_s}{dt} \qquad \text{Equation 11}$$

The settling velocity also called the terminal velocity of a falling particle is the constant velocity obtained when the drag force and buoyancy equals the gravitational force acting on the particle.[41] To calculate the vertical settling velocity for a particle the single particle Reynolds number Re_p, (Eq. 12.) is needed.

The single particle Reynolds number sets boundaries for which settling velocity term to be applied, and are divided in three groups:[42]

I $Re_p < 2$
II $2 < Re_p < 300$
III $300 < Re_p$

$$Re_p = \frac{\rho_f \, v_s \, D_p}{\mu} \qquad \text{Equation 12}$$

I $\mathbf{Re_p < 2}$

Stokes law expresses the settling velocity v_S for small spherical particles in a fluid medium. Stokes law can be seen in Eq. 13, where g is the gravitational acceleration, $\Delta\rho$ is the density difference between the particle and fluid, μ is the viscosity of the fluid and D_p is the diameter of the particle.[43] The criterion for this formula is that the single particle Reynolds number is below 2.

$$v_s = \frac{\Delta\rho \; g \; {D_p}^2}{18 \; \mu} \qquad \text{Equation 13}$$

II $\mathbf{2 < Re_p < 300}$

For a particle with a single particle Reynolds number between 2 and 300 can the settling velocity of the spherical particle be calculated from Eq. 14.[42]

$$v_s = 0.758 \cdot D_p \frac{\Delta\rho^{\frac{2}{3}}}{(\rho_f \mu)^{\frac{1}{3}}} \qquad \text{Equation 14}$$

III $\mathbf{Re_p > 300}$

For a particle with a single particle Reynolds number above 300 can the settling velocity of the spherical particle be calculated from Eq. 15.[42]

$$v_s = 3.17 \sqrt{D_p \frac{\Delta\rho}{\rho_f}} \qquad \text{Equation 15}$$

By combining the Reynolds particle number equation (with boundaries) and the corresponding settling velocity term the maximum/minimum particle diameter for the specific settling velocity term can be found. The correct vertical settling velocity for a spherical particle is found through the procedure shown in Fig. 24.

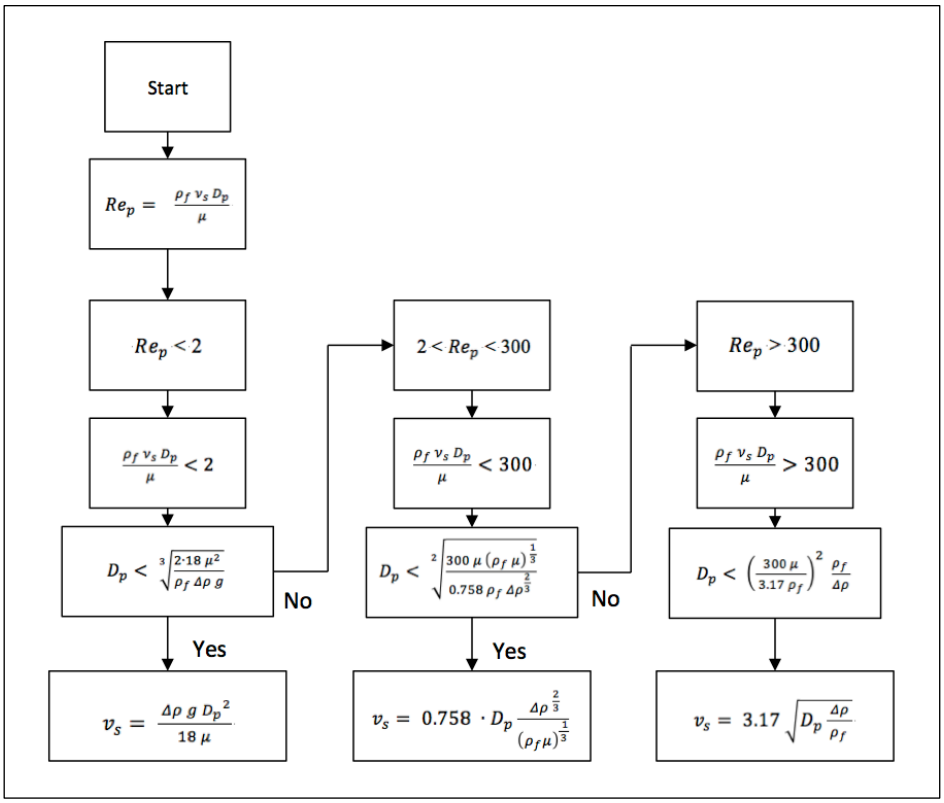

Figure 24: Procedure used to find the correct settling velocity term

5.2.2 Inclined settling velocity

As explained in the Section 3.7.2, the Boycott effect will cause an increase in settling rate in inclined tubes due to a shorter sedimentation path. When a particle rolls or slides down an inclined tube submerged in a Newtonian fluid, the particle will accelerate until the gravitational force is balanced by the resistance forces. The resistance forces include buoyancy and drag. With a decreased liquid viscosity the duration of acceleration will be longer and the value of the terminal velocity will increase.[44] The forces that apply for a spherical particle rolling down an inclined plane in a Newtonian fluid can be seen in Fig. 25.

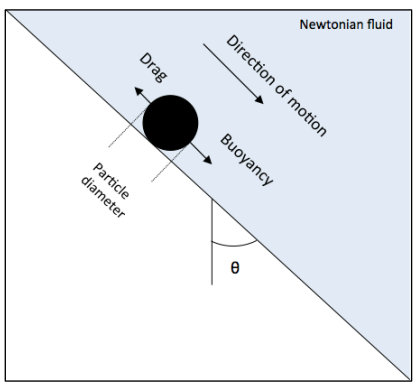

Figure 25: Sketch of the forces the applies on a spherical particle rolling on a plane in Newtonian fluid[45]

Only a few studies of the velocity of solid spherical particles that rolls or slides down an inclined tube submerged in a Newtonian fluid can be found in the literature. In 2000 Chhabra, Kumar and Prasad carried out an experimental determination of the velocity of rolling spheres in viscous fluid media as a function of the angle of inclination. The experiments where measured in smooth walled tubes with angles of inclination between 3° and 30° from the horizontal, and a sphere-tube ratio between 0.114 and 0.58. The results showed that with a sphere-tube diameter ratio above 0.5 would cause an increase in the drag coefficient.[46] An increased drag coefficient will cause an increase in drag forces and therefore decrease the particle velocity. Fig. 26 describes schematically the maximum diameter a particle can have without increasing the drag force in a tube or annulus.

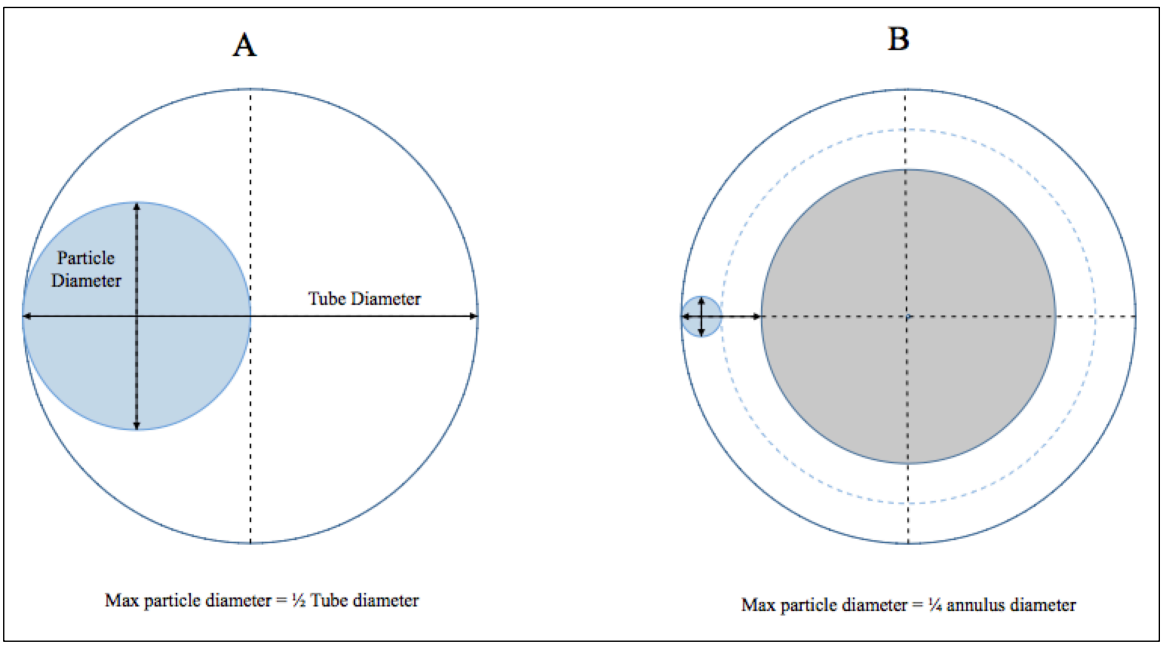

Figure 26: Maximum particle diameter in tube (A) and annulus (B)

In 2009 an analytical study on the motion of spheres rolling down an inclined plane submerged in a Newtonian fluid concluded that for an increase inclination (from the horizontal) would result in an increased terminal distance and a decreased terminal duration. The largest inclination included in this study was 30° from the horizontal plane.[45] The equation that expresses the velocity of the falling particles in this study is extensive and therefore not applicable in this thesis.

In a study by M. Jalaal and D.D. Ganji in 2011 the unsteady motion of spherical particles where studied using experimental data of Chhabra et al for a wide range of Reynolds numbers. The instantaneous particle velocity was analytically expressed through a non-perturbation series based technique called homotopy perturbation where the results showed that the inclination of the tube does not affect the acceleration duration.[44]

A simplified method can be applied to estimate the velocity settling of spherical particles in an inclined section from Eq. 16

$$v_{si} = \frac{v_s}{\cos(\theta)}$$ Equation 16

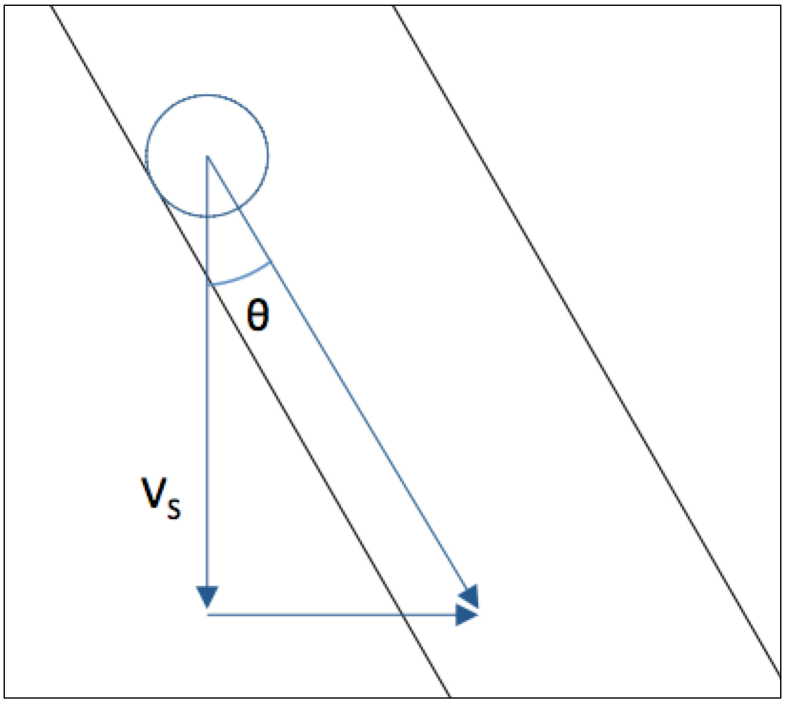

Figure 27: Sketch of vertical settling velocity in inclined well

5.3 Gravel properties

5.3.1 Gravel conductivity and permeability

The conductivity describes a materials capacity to transmit water. By looking at the gravel as a saturated media the conductivity can be measured. The closure stress is the pressure needed to close a fracture in the rock. Table 8 shows the conductivity of gravel for several closure stresses and Table 9 shows the gravel permeability, this also for several closure stresses.

	Conductivity, md-ft at 250°F				
Closure stress (psi)	**2 lb/ft²** 12/18	**2 lb/ft²** 16/20	**2 lb/ft²** 20/40	**2 lb/ft²** 30/50	**2 lb/ft²** 40/70
2,000	38,798	24,629	10,700	4,640	2,200
4,000	24,558	17,781	8,900	3,740	1,660
6,000	9,941	9,035	6,000	2,870	1,270
8,000	4,839	4,623	3,700	1,900	870
10,000	2,234	2,398	2,000	1,270	444
12,000	-	-	-	650	340

Table 8: Conductivity of gravel[22]

	Permeability, darcies at 250°F				
Closure stress (psi)	**2 lb/ft^2** 12/18	**2 lb/ft^2** 16/20	**2 lb/ft^2** 20/40	**2 lb/ft^2** 30/50	**2 lb/ft^2** 40/70
2,000	2,003	1,288	570	250	135
4,000	1,325	955	480	200	100
6,000	570	510	340	160	80
8,000	293	276	210	110	60
10,000	141	150	120	75	35
12,000	-	-	-	40	25

Table 9: Permeability of gravel[22]

5.3.2 Structural units of gravel

The rheological model proposed by Quemada in 1998 inter-particle forces where accounted for in concentrated suspensions in complex fluids. Because of these inter-particle forces, the particles formed aggregates or Structural Units (USs). Due to shear forces, the SUs are assumed to be approximately spherical and have a uniform size under steady flow condition.[47, 48] By assuming that SUs of gravel are formed as the gravel accumulates on the low-side of the well during the OHGP can the settling velocity of these SUs be determined. The SUs consist of gravel where carrier fluid occupies the gravel pore volume. A sketch of a SU can be seen in Fig. 28.

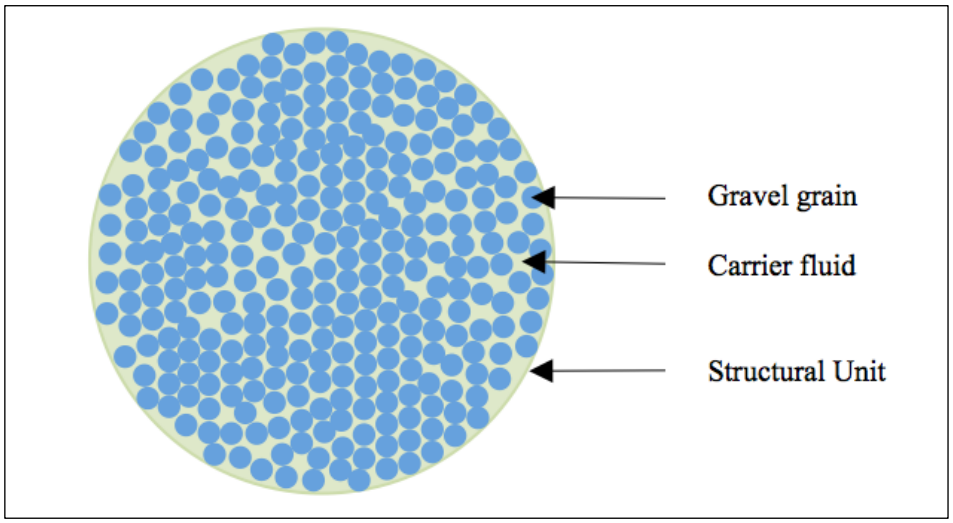

Figure 28: SU containing gravel and carrier fluid

5.4 Pressure drop

The total pressure drop inside a pipe or annulus can be broken into three different components:

- Frictional pressure drop
- Hydrostatic pressure drop
- Acceleration pressure drop

In a straight pipe or annulus with a constant cross sectional area the total pressure drop can be defined as in Eq. 17 or Eq. 18.

$$\left(\frac{dP}{dL}\right)_{total} = \left(\frac{dP}{dL}\right)_{friction} + \left(\frac{dP}{dL}\right)_{hydrostatic} + \left(\frac{dP}{dL}\right)_{acceleration} \quad \text{Equation 17}$$

$$\Delta P_{total} = \Delta P_f + \Delta P_h + \Delta P_a \quad \text{Equation 18}$$

5.4.1 Frictional pressure drop

The frictional pressure drop in a system is dependent on the flow pattern regime, velocity and wetted diameter of the pipe or OH, and describes the loss in pressure due to the friction caused by fluid flow inside a pipe. The viscous shear effect that causes this pressure loss is always positive in the direction of the flow. For a vertical or slightly inclined well the frictional pressure drop will normally contribute with 10% of the total pressured drop.[38]

The Darcy-Weisbach equation (Eq. 19) named after Henry Darcy and Julius Weisbach, is the most common equation used to calculate the frictional pressure drop and applies for all types of fully developed internal flows (independent circularity of pipe, roughness or inclination). The friction factor, f, is the Darcy-Weisbach friction factor, also named after Henry Darcy and Julius Weisbach.[49]

$$\Delta \mathrm{P}_f = f \frac{L}{D} \frac{\rho_f {v_f}^2}{2} \quad \text{Equation 19}$$

The pressure loss is often expressed in terms of the equivalent fluid column height, also called the *head loss* and is obtained by dividing the frictional pressure drop, ΔP by pg shown in Eq. 20. The head loss is caused by viscosity and is therefore directly related to the wall shear stress. The head loss represents the additional fluid height needed to overcome the frictional losses in the pipe when a fluid is to be raised by a pump.[49]

$$\mathrm{h}_L = \frac{\Delta \mathrm{P}_f}{\rho g} = f \frac{L}{D} \frac{{v_f}^2}{2g} \quad \text{Equation 20}$$

5.4.1.1 Reynolds number

The dimensionless Reynolds number for flow in a pipe or tube defined in Eq. 21 describes the ratio of the inertial forces to viscous forces, that again determines if the flow regime is either turbulent laminar or in a transition between turbulent or laminar. A laminar flow is characterized by a smooth, constant fluid flow where the viscous forces are dominant, whereas a turbulent flow is dominated by inertial forces and is characterized by chaotic eddies, vortices and other flow instabilities.[50]

$$N_{Re} = \frac{Inertial\ forces}{Viscous\ forces} = \frac{v_f D_H}{\left(\frac{\mu_f}{\rho_f}\right)} = \frac{\rho_f v_f D_H}{\mu_f}$$ Equation 21

The Reynolds number distinguishes the different flow regimes as listed below.

- Laminar flow : $N_{Re} \leq 2300$
- Transition between laminar and turbulent flow : $2300 < N_{Re} \leq 4000$
- Turbulent flow : $4000 < N_{Re}$

5.4.1.2 Friction factor

By setting the equation known as Poiseuille's law (Eq. 22), and the head loss from Eq. 20 equal to each other and then solve for *f* gives the Darcy-Weisbach friction factor for a fully developed laminar flow in a circular pipe. The Darcy-Weisbach friction factor is shown in Eq. 23 and shows that the friction factor for a laminar flow is a function of the Reynolds number and is independent of the roughness of the pipe[49].

$$v_f = \frac{\Delta P_f D^2}{32 \mu_f L}$$ Equation 22

$$f = \frac{64 \mu_f}{\rho_f v_f} = \frac{64}{N_{Re}}$$ Equation 23

The majority of flow in pipes has a turbulent flow regime, which results in a greater pressure drop compared to a laminar flow regime. The absolute wall roughness *ε,* of the pipe or OH can have a definite effect on the friction factor in a turbulent flow and thus the pressure gradient. The wall roughness of pipe is a function of pipe material, manufacture method of pipe, and the environment the pipe has been exposed to.[51]

The friction factor for a turbulent flow can be calculated from Eq. 24, proposed by Colebrook and White in 1939.[52]

$$\frac{1}{\sqrt{f}} = -2Log\left(\frac{\varepsilon}{3.7D} + \frac{2.51}{N_{Re}\sqrt{f}}\right)$$ Equation 24

Eq. 25 shows another version of Colebrook and Whites friction factor which can be rearranged into Eq. 26. As the friction factor cannot be extracted from the Colebrook equation it must be solved numerically by iterations.

$$\frac{1}{\sqrt{f}} = 1.74 - 2Log\left(\frac{2\varepsilon}{D} + \frac{18.7}{N_{Re}\sqrt{f}}\right)$$ Equation 25

$$f = \left[\frac{1}{1.74 - 2Log\left(\frac{2\varepsilon}{D} + \frac{18.7}{N_{Re}\sqrt{f}}\right)}\right]^2$$ Equation 26

The Colebrook and White equation is an accepted method for accurately estimating the friction factor for turbulent flow in pipes, but several explicit equations have been proposed in order to simplify the calculation of the friction factor. In a study done by Herbert Keith Winning and Tim Coole in 2012 a total number of 28 explicit equations were tested and compared to the Colebrook and White equation. By calculating minimum, maximum, mean relative percentage error and Mean Square Error (MSE) for the 28 equations the Buzzelli equation (Eq. 27) was the most accurate overall equation.[53, 54]

$$\frac{1}{\sqrt{f}} = A' - \left[\frac{A\prime + 2Log\left(\frac{B\prime}{N_{Re}}\right)}{1+\frac{2.18}{B\prime}}\right] \qquad \text{Equation 27}$$

Where

$$A' = [0.774ln(N_{Re})] - 1.41$$

$$B' = \left(\frac{\varepsilon N_{Re}}{3.7D}\right) + 2.51A'$$

By setting A' and B' into the Buzzelli equation the equation can be rearranged into Eq. 28.

$$f = \left[\frac{1}{([0.774ln(N_{Re})]-1.41) - \left[\frac{([0.774ln(N_{Re})]-1.41)+2Log\left(\frac{\left(\left(\frac{\varepsilon N_{Re}}{3.7D}\right)+2.51([0.774ln(N_{Re})]-1.41)\right)}{N_{Re}}\right)}{1+\frac{2.18}{\left(\left(\frac{\varepsilon N_{Re}}{3.7D}\right)+2.51([0.774ln(N_{Re})]-1.41)\right)}}\right]}\right]^2 \qquad \text{Equation 28}$$

From Eqs. 23, 24, 25 and 27 above it is clear that friction factor in a turbulent flow is dependent on both the Reynolds Number and the relative roughness $\frac{\varepsilon}{D}$, which is the ratio of the mean height of the wall roughness of the pipe and the pipe diameter.[49] The Darcy-Weisbach friction factor with Reynolds number and relative roughness for smooth and rough pipes is shown graphically in Moody's diagram in Fig. 29, plotted by Lewis Ferry Moody in 1944. [55]

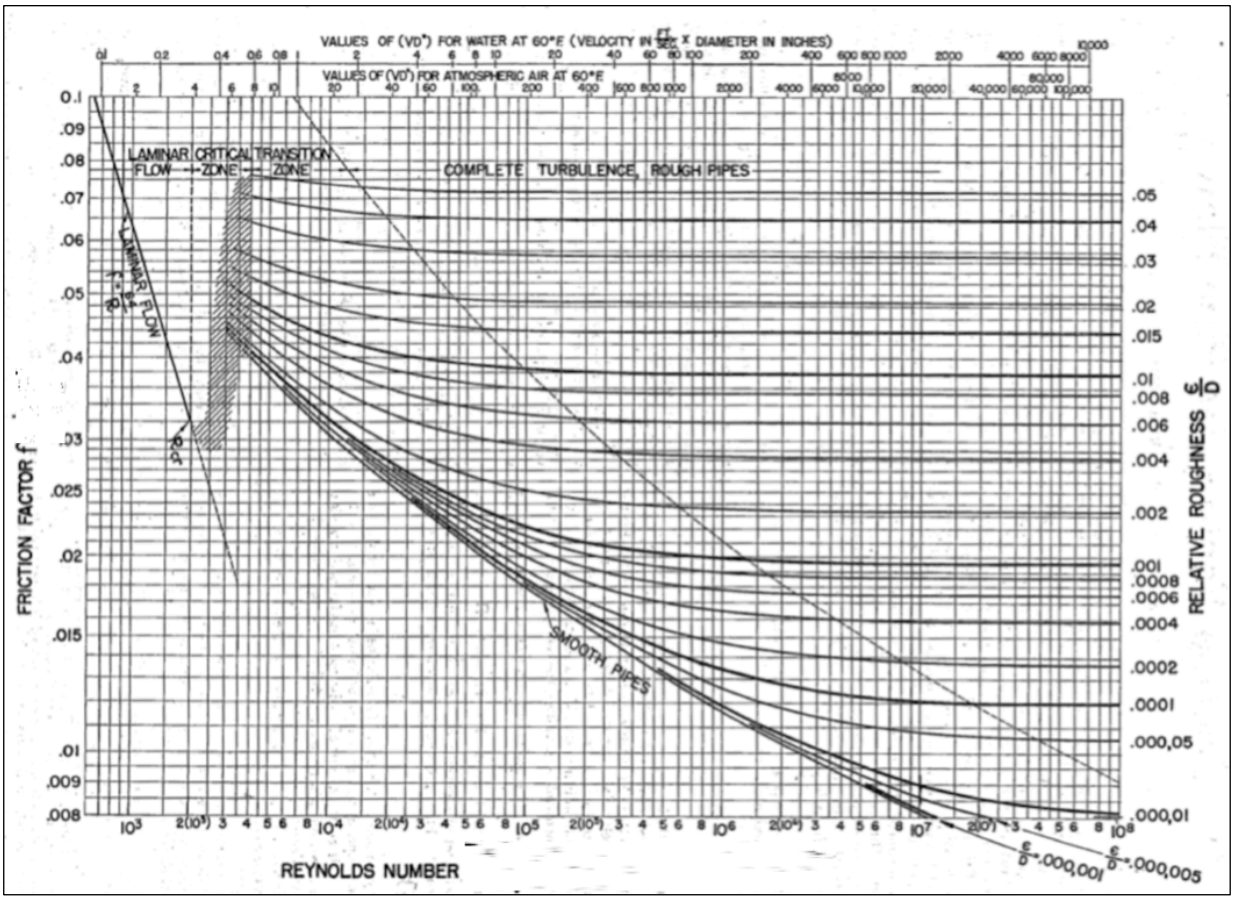

Figure 29: Moody's diagram[55]

The pipes wall roughness in the friction factor equations can sometimes be difficult to determine. Since the roughness is not a property that is physically measurable it can only be evaluated by comparing a normal pipe behavior to a sand roughened pipe. This comparison was included in Moody's results in Fig. 29, which therefore gives the Moody's diagram accepted values. The wall roughness of a pipe is as stated earlier among others a function of the environment to which it has been exposed to, and with corrosion, paraffin deposition and erosion can the relative roughness value for a pipe change significantly. If measured pressure gradients are available can the friction factor and Reynolds number be calculated and an effective relative roughness should then be used for future predictions until updated again.[51] Table 10 and 11 describes the absolute roughness for several pipe conditions and rock formations types.

Tubing/pipe condition	Surface roughness, ε	
	(in)	(m)
New tubing	0.0006	1.5240×10^{-4}
Line pipe or tubing that has been in service for some time	0.0072	1.8288×10^{-4}

Table 10: Absolute roughness of pipe/tubing[12, 51]

Rock formation types	Surface roughness, ε		
	(in)		(m)
Competent, low fracture • Igneous (e.g., granite, basalt) • Sedimentary (e.g., limestone, sandstone) • Metamorphic (e.g., gneiss)	0.12-0.24	or	0.003-0.006
Competent, medium fracture • Igneous (e.g., granite, basalt) • Sedimentary (e.g., limestone, sandstone) • Metamorphic (e.g., gneiss)	0.24-0.36	or	0.006-0.009
Poor competence, high fracture • Igneous (e.g., breccia) • Sedimentary (e.g., sandstone, shale • Metamorphic (e.g., schist)	0.02-0.04	or	0.006-0.012

Table 11: Openhole absolute surface roughness of rock[4]

5.4.2 Hydrostatic pressure drop

The hydrostatic pressure drop is the drop in pressure created when the weight of a fluid and the gravitational force is acting on a column of fluid. For a vertical or slightly inclined well the hydrostatic pressure drop will normally contribute with 80-90% of the total pressure drop. The hydrostatic pressure drop can be calculated from Eq. 29 where the inclination relative to the vertical direction is defined as θ. For a horizontal pipe the hydrostatic pressure will therefore be zero.[12, 38]

$$\Delta P_h = \rho_f g L cos\theta \qquad \text{Equation 29}$$

5.4.3 Acceleration pressure drop

The acceleration pressure drop or kinetic component represents the kinetic energy changes of the flow and is proportional to the changes in flow velocity. The acceleration pressure drop can be calculated from Eq. 30.

$$\Delta P_a = \rho_f v_f \frac{dv}{dL} \qquad \text{Equation 30}$$

For a steady incompressible flow can the kinetic energy component pressure drop caused by change in diameter be calculated from Eq. 31.[49]

$$\Delta P_a = \frac{8Q^2\rho_f}{\pi^2}\left(\frac{1}{D_2^4} - \frac{1}{D_1^4}\right) \qquad \text{Equation 31}$$

5.5 Pressure drop gradient balance and flow split

When slurry flows pass a screen section a flow split will occur: a certain amount of carrier fluid will choose to flow through the screen and down the mini-annulus between the screen and the WP rather than in the annulus between OH and screen (together with the rest of the slurry). This means that the slurry density originally pumped down the well is denser after passing the upper screen section due to the loss of carrier fluid, which again affects the settling. The amount of carrier fluid that chooses to flow through the screen and down mini-annulus is dependent on pressure and the effective inlet area of the wire-wrapped screen.

With a known wire height h_w, and the screen gauge the percentage of the open area of the screen can be calculated as shown in Eq. 32. With this knowledge can Eq. 33 be used to calculate the flow area per foot for the screen.

$$\%\ Open\ area\ = \frac{\frac{Screen\ gauge}{1000}}{h_w + \frac{Screen\ gauge}{1000}} \cdot 100 \qquad \text{Equation 32}$$

$$Screen\ opening\ \left[\frac{in^2}{ft}\right] = D_s \cdot \pi \cdot (\%\ open\ area) \cdot 12\ \frac{in}{ft} \qquad \text{Equation 33}$$

With a split flow between annulus and mini-annulus a pressure drop balance equation (Eq. 36) can be used to calculate the two flow rates. This is done by using trial and error until the two pressure drops are equal. The hydrostatic pressure gradient for these two annuli will be the same if the density of the fluids is the same in both annuli, and can therefore be neglected when calculating the pressure drop balance.

$$\left(\frac{dP}{dL}\right)_{Annulus} = \left(\frac{dP}{dL}\right)_{Mini-annulus} \qquad \text{Equation 34}$$

$$\left(\frac{\Delta P_h + \Delta P_f}{L}\right)_{Annulus} = \frac{\left(\Delta P_h + \Delta P_f\right)}{L}_{Mini-annulus} \qquad \text{Equation 35}$$

$$\left(\rho_f g cos\theta + f\frac{\rho_f {v_f}^2}{D2}\right)_{Annulus} = \left(\rho_f g cos\theta + f\frac{\rho_f {v_f}^2}{D2}\right)_{Mini-annulus} \qquad \text{Equation 36}$$

6. CALCULATION AND DISCUSSION

In order to calculate the settling of gravel in this thesis a certain set of parameters was needed. A well on the Norwegian sector has been chosen as a basis for the calculations as mentioned earlier. In this chapter the calculations for this thesis will be carried out.

6.1 Well data

The field data for the well that is used as a basis for the calculations in this thesis can be seen in Table 12, and the completion data for the modified well can be seen in Table 13.

Well Data	:							
Depth (TVD)	:			2,504	m			
Depth (MD)	:			2,571	m			
Inclination	:	0.523598776	Rad	30	Deg			
Openhole	:	8.5	in	0.2159	m			
BHP (Bottom hole pressure)	:	168	bar					
BHT (Bottom hole temperature)	:	80	C	≈50 when circulating			353.15	K
Pump rate	:	1,100	LPM	1.1	m^3/min			
Absolute Roughness	:							
ε Openhole	:	0.04000	ft	0.48	in		0.0122	m
ε Drillpipe - Casing	:	0.00075	ft	0.009	in		0.0002286	m
ε Washpipe - Mini-annulus	:	0.00060	ft	0.0072	in		0.00018288	m
Casing	:							
OD	:	9.625	in	0.244475	m			
ID	:	8.535	in	0.216789	m			
Drillpipe	:							
OD	:	5.000	in	0.127	m			
ID	:	4.2700	in	0.108458	m			
Screen (12 gauge)	:							
OD	:	6.1	in	0.15494	m			
ID	:	4.778	in	0.1213612	m			
Wire height		0.12	in	0.003048	m			
Basepipe	:							
OD	:	5.5	in	0.1397	m			
ID	:	4.778	in	0.1213612	m			
Washpipe	:							
OD	:	4	in	0.1016	m			
ID	:	3.548	in	0.0901192	m			
Gravel (20/40 U.S. Mesh)	:							
Median particle diameter	:	730	µm	0.0007300	m			
Permeability @250 F		695	Darcy	0.000000695	m^2			
Conductivity		13,040	mD-ft	0.000000013	m^2/ft			
Concentration	:	90	kg/min	81.818	kg/m^3			
Density	:	2.71	SG	2,710.000	kg/m^3			
Bulk Density	:	1.57	SG	1,570.000	kg/m^3			
Carrier Fluid ($NaCl_2$)	:							
Density	:	1.2	SG	1,200	kg/m^3			
Viscosity @ 50 °C	:	1.527	cP	0.001527	kg/m-s			

Table 12: Well data

Vertical section				
Drillpipe	Length 2,071 m			
	Top 0 m			
	Bottom 2,071 m			
Inclined section				
Inclination from the vertical	0.524 Rad			
	30 Deg			
Drillpipe	Length 111 m			
	Top 2,071 MD			
	Bottom 2,182			
Upper screen section	Length 80 m			
	Top 2,182 MD			
	Bottom 2,262 MD	**OH section**	Length 389 m	
Blank Pipe section	Length 229 m		Top 2,182 MD	
	Top 2,262 MD		Bottom 2,571 MD	
	Bottom 2,491 MD			
Lower screen section	Length 80 m			
	Top 2,491 MD			
	Bottom 2,571 MD			
Total	Length 500 m			
	Top 2,071 MD	**Total length (TVD)**	2,504 m	
	Bottom 2,571 MD	**Total length (MD)**	2,571 m	

Table 13: Completion data for modified well

6.1.1 Carrier fluid viscosity

The viscosity of the carrier fluid is a crucial parameter when calculating the fluid flow and particle settling. The viscosity of fresh water and sodium chloride brine gathered from Halliburton's simulator data can be seen in Table 14.

Fresh water, H_20 SG: 1.00		**Sodium Chloride, NaCl** SG: 1.200			
Temperature (°C)	Viscosity (cp)	Temperature (°C)	1 Atm	300 bar	400 bar
10	1.3080	0	2.775	2.710	2.693
20	1.0020	10	2.284	2.257	2.250
30	0.7978	20	1.978	1.968	1.966
40	0.6531	30	1.772	1.771	1.772
50	0.5471	40	1.627	1.631	1.632
60	0.4668	50	1.521	1.527	1.529
70	0.4044	60	1.440	1.447	1.450
80	0.3550	70	1.378	1.385	1.388
90	0.3150	80	1.328	1.336	1.339
100	0.2822	90	1.288	1.296	1.299
		100	0.0122	1.263	1.266
		110	0.0126	1.236	1.239

Table 14: Viscosity of Sodium Chloride brine and fresh water

6.1.2 Slurry density

The density of the slurry can be calculated from Eq. 37.

$$\rho_{\text{slurry}} = \frac{m_g v_g + m_b v_b}{v_g + v_b} \qquad \text{Equation 37}$$

Eq. 38 can also be used as a starting point for density calculations for the slurry since the mass flow rate of the slurry always will be the sum of the gravel and carrier fluids mass flow rate. By combining Eq. 38 and Eq. 39 the slurry density can be calculated from Eq. 40.

$$\dot{m}_{\text{slurry}} = \dot{m}_g + \dot{m}_b \qquad \text{Equation 38}$$

$$\dot{m} = \rho \cdot Q \qquad \text{Equation 39}$$

$$\rho_{\text{slurry}} = \frac{\rho_b Q_b + \rho_g Q_g}{Q_{\text{slurry}}} \qquad \text{Equation 40}$$

Gravel rate

With 90 kg of gravel added to the CLAM per minute and a gravel density of 2,710 kg/m^3 gives a volumetric rate Q_g, of:

$$Q_g = \frac{\dot{m}_g}{\rho_g} = \frac{90\frac{kg}{min}}{2{,}710\frac{kg}{m^3}} = 0.03321\,\frac{m^3}{min} \qquad \text{Equation 41}$$

Brine rate

With a slurry pump rate of 1.100 m^3/min gives a brine rate Q_b, of:

$$Q_b = Q_{\text{slurry}} - Q_g = 1.100\,\frac{m^3}{min} - 0.03321\,\frac{m^3}{min} = 1.06679\,\frac{m^3}{min}$$

Slurry density

By applying Eq. 40 will give a slurry density ρ_{slurry}, of:

$$\rho_{\text{slurry}} = \frac{\left(2{,}710\frac{kg}{m^3} \cdot 0.03321\frac{m^3}{min}\right) + \left(1{,}200\,\frac{kg}{m^3} \cdot 1.06679\frac{m^3}{min}\right)}{1.100\,\frac{m^3}{min}} = 1{,}245.588\ \frac{kg}{m^3}$$

$$\approx 1.246\ SG$$

6.1.3 Screen opening, gravel conductivity and gravel permeability

With a 20/40 U.S. mesh size on the gravel it can be seen from Table 5 that a screen size of 0.012 inches (12 gauges) is sufficient to both hold the gravel in place and to minimize the restriction of fluid flow and interstitial fines.

By recalling Eq. 32 the open area percentage of the wire wrapped screen will be as follows:

$$\%\ Open\ area\ = \frac{\frac{12}{1000}in}{0.12in + \frac{12}{1000}in} \cdot 100 = 9.091\%$$

Eq. 33 then gives a screen opening or inlet area of:

$$Screen\ opening\ \left[\frac{in^2}{ft}\right] = 6.1in\ \cdot \pi \cdot 9.091\% \cdot 12\frac{in}{ft} = 20.906\frac{in^2}{ft}$$

The conductivity of the gravel from Table 8, and the permeability of gravel from Table 9 can be plotted against the closure stress shown in Fig. 30 and Fig. 31. By setting a linear trendline it is possible to calculate the permeability and conductivity for a closure stress of zero psi. As the closure stress is the pressure used for hydraulic fracturing and this thesis revolves an OHGP will a closure stress of zero psi be the most correct value to use. This gives a gravel permeability of 695 Darcy, and a gravel conductivity of 13,040 mD-ft.

The permeability data is used to calculate the fluid flow through a gravel pack. As mentioned earlier will a certain percentage of the carrier fluid flow through the packed gravel in the lower screen section instead of flowing upwards to the upper screen section. The rate of this fluid flow can be calculated here in addition to the pressure drop.

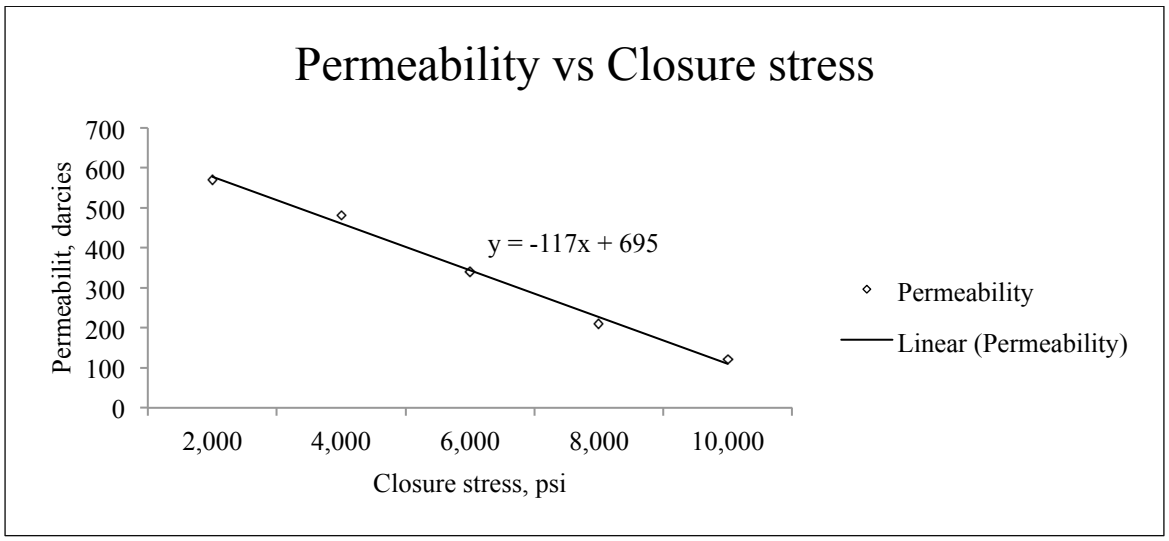

Figure 30: Permeability of 20/40 U.S. mesh gravel plotted against closure stress

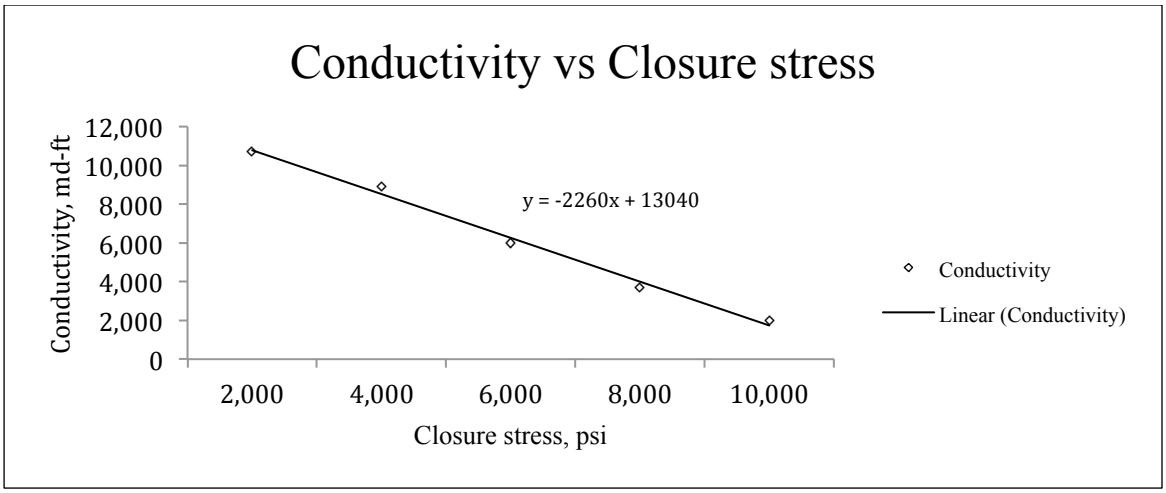

Figure 31: Conductivity of 20/40 U.S. mesh gravel plotted against closure stress

6.1.4 Volume calculations

Calculating the exact volume of gravel needed for the OHGP is necessary in order to determine whether the well has been sufficiently packed or not. In addition to the volume of gravel that is to be packed in blank pipe and screen sections is an extra volume of gravel needed in the slurry that remains in the drillpipe when screeenout is a factum. Since the gravel is spherical it is necessary to calculate the volume fraction of gravel in a packed gravel bed. Brine will fill the pore volume of the gravel grains. With a known bulk volume of the gravel the volume fraction of gravel V_{fg}, and the volume fraction of brine V_{fb}, in a gravel bed can be calculated as follows:

$$V_{fg} = \frac{\rho_{bg}}{\rho_g} = \frac{1{,}570\,\frac{kg}{m^3}}{2{,}710\frac{kg}{m^3}} = 0.5793 \qquad \text{Equation 42}$$

$$V_{fb} = 1 - V_{fg} = 1 - 0.5793 = 0.4207 \qquad \text{Equation 43}$$

The density of a gravel packed bed ρ_{gb}, can be calculated from Eq. 44.

$$\rho_{gb} = \left(V_{fg} \cdot \rho_g\right) + \left(V_{fb} \cdot \rho_b\right) \qquad \text{Equation 44}$$
$$= \left(0.5793 \cdot 2{,}710\,\frac{kg}{m^3}\right) + \left(0.4207 \cdot 1{,}200\,\frac{kg}{m^3}\right)$$
$$= 2{,}074.8\,\frac{kg}{m^3}$$

The volume of gravel needed is equal to the volume fraction of gravel multiplied by the volume in the annulus between OH and screen/BP, plus the additional gravel in the slurry that remains in the drillpipe after screenout. The volume of gravel needed for the different sections in the well can be seen in Table 15. The amount of gravel that remains in drillpipe after screenout is calculated form the Eq. 45.

$$V_g = \frac{V_{DP}\left(\frac{\dot{m}_g}{Q_{slurry}}\right)}{\rho_g} = \frac{20.1588\ m^3\left(\frac{90\frac{kg}{min}}{1.1\frac{m^3}{min}}\right)}{2{,}710\ \frac{kg}{m^3}} = 0.60862\ m^3$$ Equation 45

Section		Cross sectional area	Length	Volume	Volume gravel needed	Volume slurry needed
		m^2	m	m^3	m^3	m^3
OH-Screen (Upper)	:	0.01776	80	1.42040	0.82289	27.2559
OH-Screen (Lower)	:	0.01776	80	1.42040	0.82289	27.2559
OH-BP	:	0.02128	229	4.87351	2.82340	93.5173
Drillpipe	:	0.00924	2,182	20.1588	0.60862	20.1588
Total				27.87315	5.07780	168.1880

Table 15: Volume of gravel needed for OHGP

6.2 Pressure calculations

The pressure calculations needed for the modified well are developed in this section. The surface treating pressure or pump pressure describes graphically the gravel placement versus pumping time, and can with assumptions be predicted. Pressure calculations are needed for flow split determination between annulus and mini-annulus. Eq. 21 is used to calculate the Reynolds Number. The frictional pressure drop is calculated from Eq. 19, where Eq. 23 is used to find the friction factor for laminar flow, and Eq. 27 is used to find the friction factor for turbulent flow. The hydrostatic pressure drop is calculated using Eq. 29, and the pressure drop balance gradient is calculated from Eq. 34.

6.2.1 Wellbore segmentations and sign convention of pressure drop

By dividing the different segments of the wellbore into groups simplifies the pressure calculations. From Fig. 32 it can be seen that the pressure drop is divided into a combined vertical and inclined section group and an inclined section group. The pressure sign conventions for each segment can be seen below each segment in the same figure.

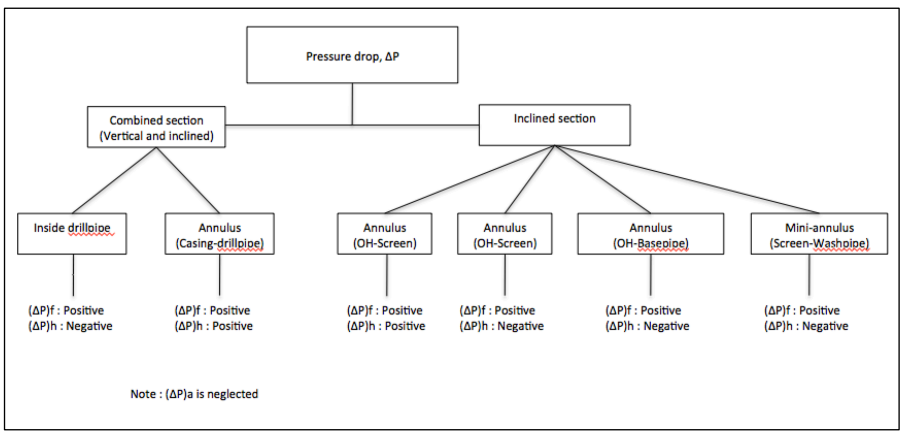

Figure 32: Wellbore segmentation and sign convention of pressure drop

6.2.2 Pumping slurry down the drillpipe

The pressure drop from the displacement of carrier fluid with slurry in the drillpipe is the first pressure drop that can be seen on the surface treating pressure graph. The slurry is pumped down the drill pipe and fills up the entire section above OH. Since there is no flow split in the drillpipe the slurry will have the same flow rate as the pump rate. As slurry is pumped down the drillpipe the pre-existing carrier fluid in the drillpipe will flow through the crossover tool and out the crossover ports to annulus.

The result of trial and error to balance the pressure drop between annulus and mini-annulus can be seen in Table 16. The table shows that 82.174% of the fluid rate will go down annulus between the OH and the screen.

Annulus (OH-D_S)				**Mini-annulus (D_{SI}-D_{WP})**			
Pump rate	1.1000	m^3/min		Pump rate	1.1000	m^3/min	
Flow area	0.0178	m^2		Flow area	0.0035	m^2	
D_H	0.0610	m	%	D_H	0.0198	m	%
Q_a	0.9039	m^3/min	82.174	Q_{ma}	0.1961	m^3/min	17.825
Q_a	0.0151	m^3/s		Q_{ma}	0.0033	m^3/s	
Velocity actual	0.8485	m/s		Velocity actual	0.9444	m/s	
Viscosity	0.0015	kg/m-s					
N_{Re}	40,649	TURBULENT		N_{Re}	14,665	TURBULENT	
Absolute roughness	0.0122	m		Absolute roughness	0.0002	m	
Buzzelli friction factor	*A'*	*B'*	*f*	Buzzelli friction factor	*A'*	*B'*	*f*
	6.8042	2,214.3	0.1560		6.0152	51.780	0.0408
Density	1,200.0	kg/m^3		Density	1,200.0	kg/m^3	
$(\Delta P/L)_f$	1,105.4	Pa/m		$(\Delta P/L)_f$	1,105.4	Pa/m	
$(\Delta P/L)_f$	0.01105	Bar/m		$(\Delta P/L)_f$	0.01105	Bar/m	

Table 16: Pressure drop gradient balance for flow split between annulus and mini-annulus when slurry is pumped down the drillpipe

The time it takes for the slurry to fill up the drillpipe above OH is calculated as in the Eq. 46.

$$T_P = \frac{V_{DP}}{Q_P} = \frac{20.1588\ m^3}{1.1\ \frac{m^3}{min}} = 18.326\ min \qquad \text{Equation 46}$$

6.3 Gravel packing the modified well

6.3.1 Scenario 1: Gravel packing lower screen section

The flow split that occurs between annulus and min-annulus when slurry is pumped down the well has been calculated from the pressure drop balance gradient from Eq. 34. The flow split calculation can be seen in Table 17 and shows that 84.574% of the slurry will continue to flow down annulus, whereas the remaining 15.426%, (this being carrier fluid) will flow through the upper screen and down mini-annulus.

The slurry that chooses to flow down annulus is now denser than the original slurry due to the flow split. With a slurry rate of 0.9393 m^3/min from Table 17 and a concentration of 90 kg/min gravel gives a slurry density of 1,253.9 kg/m^3. The slurry will eventually reach the lower screen section where the gravel starts to pack off. The remaining carrier fluid in the slurry will flow through the lower screen and up WP to surface. When a certain volume of gravel settles in the bottom of the will the same volume of carrier fluid will be displaced. This additional volume of carrier fluid will as the rest of the carrier fluid flow through the screen, up WP and up to surface making a total flow rate of 1.1 m^3/min.

Annulus (OH-D_S)				**Mini-annulus (D_{SI}-D_{WP})**			
Pump rate	1.1000	m^3/min		Pump rate	1.1000	m^3/min	
Flow area	0.0178	m^2		Flow area	0.0035	m^2	
D_H	0.0610	m	%	D_H	0.0198	m	%
Q_a	0.9303	m^3/min	84.574	Q_{ma}	0.1697	m^3/min	15.426
Q_a	0.0155	m^3/s		Q_{ma}	0.0028	m^3/s	
Velocity actual	0.8733	m/s		Velocity actual	0.8172	m/s	
Viscosity	0.0015	kg/m-s		Viscosity	0.0015	kg/m-s	
N_{Re}	43,425	TURBULENT		N_{Re}	14,665	TURBULENT	
Absolute roughness	0.0122	m		Absolute roughness	0.0002	m	
Density	1,245.6	kg/m^3		Density	1,200.0	kg/m^3	
Buzzelli friction factor	*A'*	*B'*	*f*	Buzzelli friction factor	*A'*	*B'*	*f*
	6.8554	2,364.50	0.1560		6.0152	51.78	0.0408
Frictional				**Frictional**			
$(\Delta P/L)_f$	1,215.33	pa/m		$(\Delta P/L)_f$	827.91	pa/m	
$(\Delta P/L)_f$	0.01215	bar/m		$(\Delta P/L)_f$	0.0083	bar/m	
Hydrostatic				**Hydrostatic**			
Inclination	0,5236	rad	30 Deg	Inclination	0.5236	rad	30 Deg
g	9.81287	m/s^2		g	9.81287	m/s^2	
$(\Delta P/L)_h$	-	Pa/m		$(\Delta P/L)_h$	-	Pa/m	
$(\Delta P/L)_h$	-	Bar/m		$(\Delta P/L)_h$	-	bar/m	
$(\Delta P/L)_{total}$	-9,369.2	Pa/m		$(\Delta P/L)_{total}$	-9,369.9	Pa/m	
$((\Delta P/L)_{total}$	-0.09370	Bar/m		$(\Delta P/L)_{total}$	-0.09370	Bar/m	

Table 17: Pressure drop gradient balance for flow split between annulus and mini-annulus when packing lower screen section

It takes 6.765 minutes to fill the upper screen section and blank pipe section with slurry. Calculation on pumping time can be seen in Eq. 47.

$$T_P = \frac{V_{OH-Screen} + V_{OH-BP}}{Q_a} = \frac{1.42040\ m^3 + 4.87351\ m^3}{0.9303\ \frac{m^3}{min}} = 6.765\ min \qquad \text{Equation 47}$$

The volumetric calculations in Table 15 shows that a volume of 0.82289 m^3 gravel is needed to pack the lower screen section. With a gravel concentration of 90 kg/m^3 a pumping time of 24.778 minutes is required to pack the lower screen. Calculation on pumping time for this section can be seen in Eq. 48.

$$T_P = \frac{V_g\ needed}{\left(\frac{\dot{m}_g}{\rho_g}\right)} = \frac{0.82289\ m^3}{\left(\frac{90\ \frac{kg}{m^3}}{2{,}710\ \frac{kg}{m^3}}\right)} = 24.778\ min$$ Equation 48

6.3.2 Scenario 2: Gravel packing blank pipe section

During packing of the lower screen section in "Scenario 1" the slurry density in annulus is increased to 1,253.9 kg/m^3 due to a flow split. When the lower screen section is packed with gravel it will be a column of slurry with the same increased density placed in the blank pipe section. The gravel in this column of slurry settles down and takes up a certain volume of the blank pipe section. This occupied volume in the blank pipe section must be taking into account during calculations on the total settling time.

When spherical particles like gravel slides down an inclined tube filled with a Newtonian fluid like brine, the particles will obtain acceleration. In order to calculate the actual settling velocity and acceleration further tests and experiments needs to be carried out. A simplified model has therefore been used to estimate the settling velocity in the blank pipe section.

A theoretical model is used when determining the velocity of the gravel that slides down the lower side of the well. The theoretical model can be seen in Fig. 33, and shows that the gravel is placed in horizontal layers over time until the blank pipe section is completely packed with gravel. From this model the average gravel settling velocity can be determined. Fig. 34 illustrates the Boycott effect where the gravel slides down on the lower side, where the gravel is placed in slope-shaped layers. The dissimilar shape on the gravel packed layers for the two models has an effect on the packing percentage for a certain height at time t. In other words, the total volume of gravel in the well will be the same for both models at time t, but the distribution of gravel is different. A comparison of the two models based on Fig. 33 and Fig. 34 can be seen in Table 18.

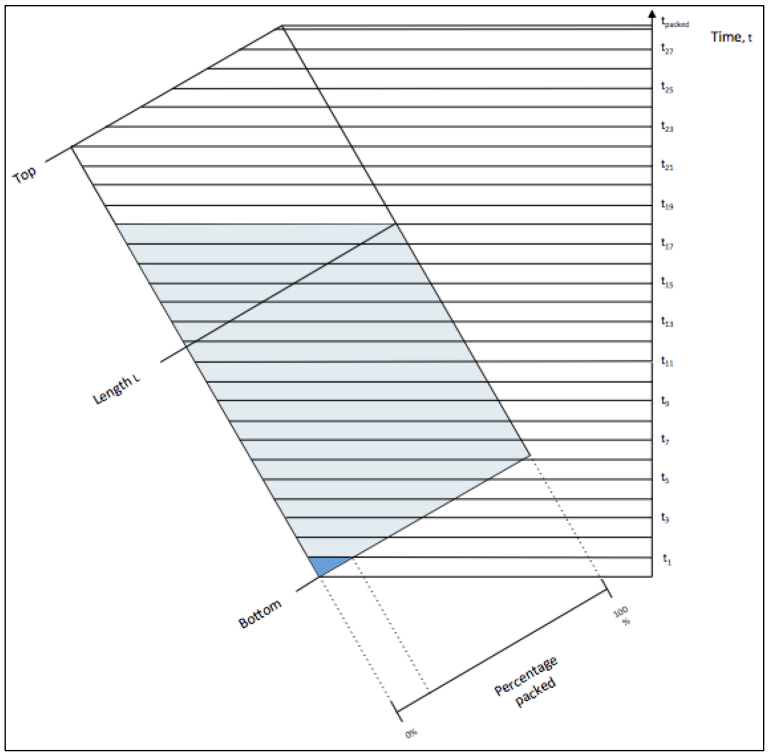

Figure 33: Theoretical model of gravel placement in blank pipe section

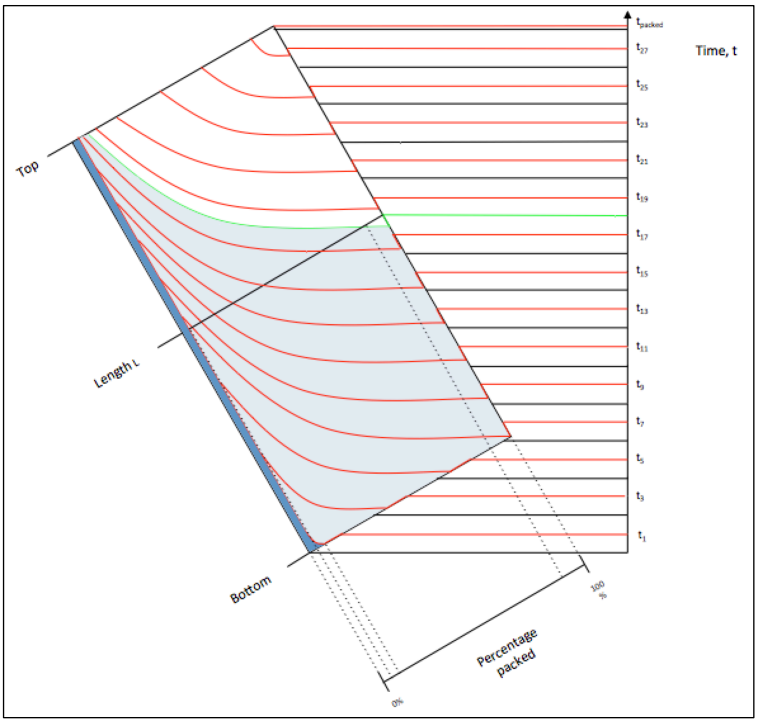

Figure 34: Boycott model of gravel placement in blank pipe section

At time, t Model	t_1 Theoretical model	t_1 Boycott model	t_{18} Theoretical model	t_{18} Boycott model
Percentage of bottom filled with gravel	14.29	7.79	100	100
Total volume of gravel in well	A	A	B	B
Percentage of "L" filled with gravel	0	5.19	100	88.96
Total volume of gravel in well	A	A	B	B

Table 18: Comparison of theoretical model and Boycott model for gravel placement in blank pipe section

With an inclined blank section it can be seen in both the theoretical model and the boycott model that when gravel starts to settle and pack the bottom low-side of the well there will be a open area on the bottom high-side of the well. This means that in the Boycott model (Fig. 34), the carrier fluid will flow through the underlying screen until the high-side of the bottom blank pipe section is packed with gravel at time $t_{7...}$ In other words, the lower screen section is not sufficiently packed until time t_7, in the blank pipe section.

6.3.2.1 Calculation based on pump rate

The accumulation of gravel on the lower side on the inclined tube is filled with brine in the open gravel pore space. This volume of packed gravel will slide down the lower side until it reaches the bottom of the blank section. Based on the pump rate a packing rate Q_p, can be calculated from Eq. 49.

$$Q_p = \frac{Q_g}{V_{fg}} = \frac{0.03321 \frac{m^3}{min}}{0.5793} = 0.0573 \frac{m^3}{min} \qquad \text{Equation 49}$$

By taking the basis in one minute the volume of brine occupying the pores in the packed gravel V_{bgp}, will be:

$$\begin{aligned} V_{bgp} &= V_{fg} \cdot Q_p \cdot T_P \\ &= 0.4207 \cdot 0.0573 \frac{m^3}{min} \cdot 1\, min \\ &= 0.02411\, m^3 \end{aligned}$$

The amount of brine that flows directly through the upper screen V_{bs}, in one minute then is:

$$\begin{aligned} V_{bs} &= (Q_b \cdot T_P) - V_{bgp} \\ &= \left(1.06679 \frac{m^3}{min} \cdot 1\, min\right) - 0.02411\, m^3 \\ &= 1.0426\, m^3 \end{aligned}$$

A packing rate of 0.0573 m^3/min will displace the same rate of brine, making a total of 1.1 m^3/min brine flowing up to surface.

With a known V_{bgp} and V_{bs} per minute gives the following volume fractions respectively:

$$V_{fpg} = \frac{Q_{\mathrm{p}}}{Q_{\mathrm{P}}} = \frac{0.0573\,\frac{m^3}{min}}{1.1\,\frac{m^3}{min}} = 0.0521$$

$$V_{fbs} = \frac{V_{bs}}{Q_{\mathrm{P}} \cdot T_P} = \frac{1.0426\,m^3}{1.1\,\frac{m^3}{min} \cdot 1\,min} = 0.9478$$

The total volume of blank pipe section that is to be packed due to gravel settling is equal to the volume of annulus between OH and BP minus the gravel from the preexisting column of gravel in slurry that is placed in the blank pipe section when the lower screen section was packed. The length of the blank pipe section that is packed due to gravel that settles freely is 217.06601 m. The calculation can be seen in Eq. 50

$$\begin{aligned} L &= \frac{V_{OH-BP} - (V_{OH-BP} \cdot V_{fpg})}{A_{OH-BP}} \\ &= \frac{4.87352\ m^3 - (4.87352\ m^3 \cdot 0.0521)}{0.02128\,m^2} \\ &= 217.06601\ \mathrm{m} \end{aligned} \qquad \text{Equation 50}$$

The volumetric calculations in Table 15 shows that a theoretical volume of 4.87352 m^3 is to be packed in the blank pipe section. A packing rate Q_{pr}, of 0.0573 m^3/min requires a pumping time T_P, of 80.6 minutes in order to gravel pack the entire section. The calculation on pumping time for this section can be seen in Eq. 51.

$$T_P = \frac{V_{OH-BP} - (V_{OH-BP} \cdot V_{fpg})}{Q_p} = \frac{4.87352\ m^3 - (4.87352\ m^3 \cdot 0.0521)}{0.0573\,\frac{m^3}{min}} = 80.6\,min \qquad \text{Equation 51}$$

6.3.2.2 Calculation of settling velocity of structural units

By making the rough assumption that SUs behaving as solid spheres of gravel will achieve its terminal velocity instantaneously can the settling velocity be calculated from the single particle settling terms in Section 5.2.

The maximum diameter a SU can have without increasing the drag forces, equals ¼ of the annulus diameter as presented in Section 5.2.2. This gives a SU diameter D_{SU} of:

$$D_{SU} = \frac{1}{4}\,(\mathrm{D_{OH}} - \mathrm{D_{BP}}) = \frac{0.2159\,m - 0.1397\,m}{4} = 0.01905\,m \qquad \text{Equation 52}$$

The volume of one SU V_{SU}, can be calculated:

$$V_{SU} = \frac{\pi}{6}\,(D_{SU})^3 = \frac{\pi}{6}\,(0.01905\,m)^3 = 3.61979 \cdot 10^{-6}\,m^3 \qquad \text{Equation 53}$$

By following the procedure in Fig. 24 calculations show that with a SU diameter of 0.01905 m the correct settling velocity term to use is Eq. 15. The settling velocity for a single SU for a vertical section will then be:

$$v_s = 3.17\sqrt{D_p\frac{\Delta\rho}{\rho_f}} = 3.17\sqrt{0.01905\,m\;\frac{2074.8\frac{kg}{m^3}-1{,}200\frac{kg}{m^3}}{1{,}200\frac{kg}{m^3}}} = 0.3736\frac{m}{s}$$

By recalling Eq. 16 gives a settling velocity for a single SU in the inclined blank section of:

$$v_{SU} = \frac{v_s}{\cos(\theta)} = \frac{0.3736\frac{m}{s}}{\cos(30)} = 0.4314\;\frac{m}{s}$$

$$= 25.8815\;\frac{m}{min}$$

With SUs sliding down on the low-side lined as shown in Fig. 35 the center-to-center length for two SUs will be equal to the SU's diameter $D_{SU.}$ The placement of SU number *n* in relation to the section length can be calculated from Eq. 54.

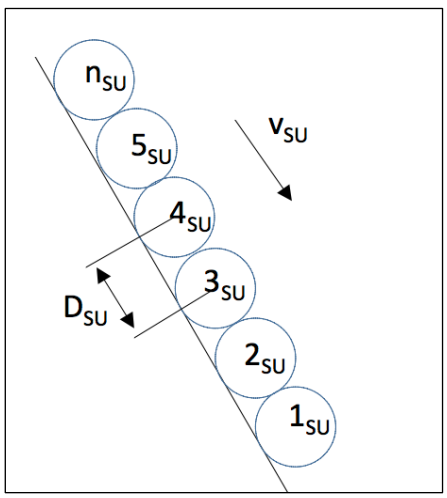

Figure 35: SUs sliding on low-side of blank pipe section lined

$$n_{SU} = 1_{SU} - D_{SU}\cdot(n-1) \qquad \text{Equation 54}$$

The average cross sectional area that is packed over time during the OHGP in the blank pipe section in the theoretical model is equal to the cross sectional area between OH and BP: $A_{OH\text{-}BP.}$ The number of SUs needed to cover this cross sectional area is calculated from the circumference of OH and BP:

$$N_{SU} = \frac{C_{OH}+C_{BP}}{D_{BP}} = \frac{\pi(D_{OH}+D_{BP})}{D_{BP}} = \frac{\pi\,(0.2159\,m+0.1397\,m)}{0.01905\,m} = 58.64$$

There is not enough space for 59 SUs in the cross sectional and 58 CUs are therefore used to achieve one layer of CUs. A scaled sketch of one layer of SUs can be seen in Fig. 36.

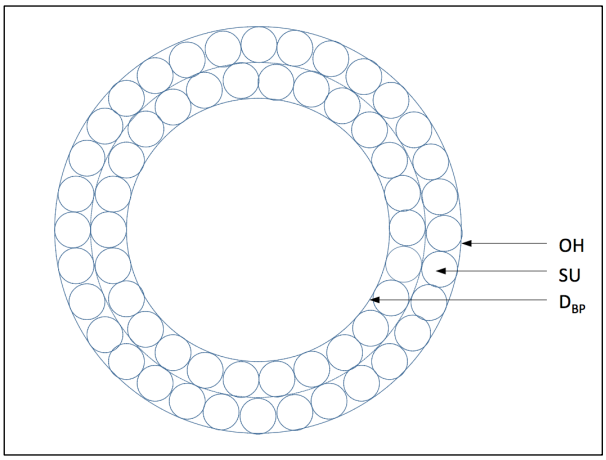

Figure 36: Scaled sketch of one layer of SUs seen from above

With 58 SUs in one layer can the layer height h_{layer}, be calculated from Eq. 55

$$h_{layer} = \frac{V_{SU} \cdot N_{SU}}{A_{OH-BP}} \cdot \frac{V_{SU} \cdot N_{SU}}{\frac{\pi(D_{OH}{}^2 - D_{BP}{}^2)}{4}} = \frac{3.61979 \cdot 10^{-6}\ m^3 \cdot 58}{\frac{\pi((0.2159\ m)^2 - (0.1397\ m)^2)}{4}} = 0.009865\ \text{m} \qquad \text{Equation 55}$$

A layer height of 0.009865 m gives an additional length L_a for the next SU to settle before a new layer of SUs can be made. This additional length is illustrated in Fig. 37 and the additional time t_a, needed for a SU to settle this length is calculated from Eq. 56.

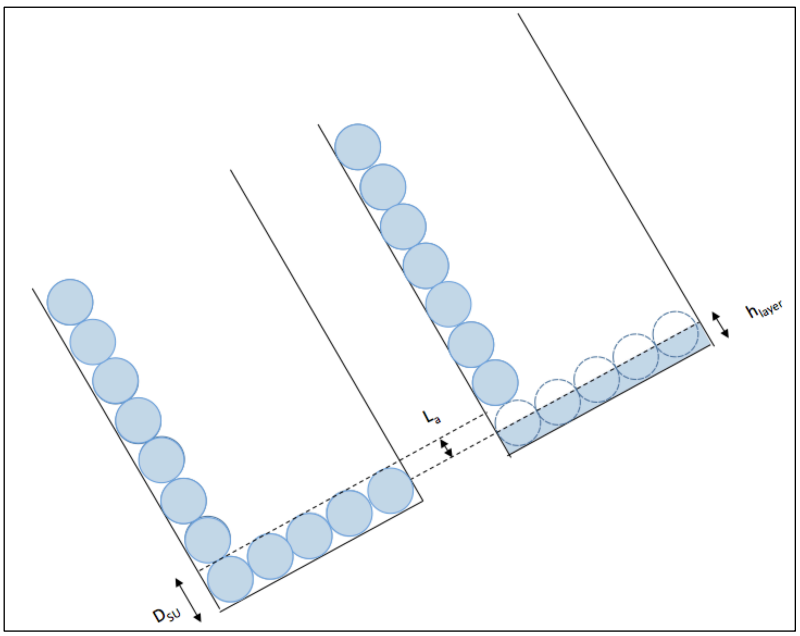

Figure 37: Additional length L_a, for a SU to settle before a new layer can be made

$$t_a = \frac{D_{SU} - h_{layer}}{v_{SU}} = \frac{0.01905\ m - 0.009865\ m}{0.4314\ \frac{m}{s}} = 0.021293\ s \qquad \text{Equation 56}$$

Table 19 shows the position of 1_{SU}, 2_{SU}, 3_{SU} and 58_{SU} relative to the blank pipe section over time. Time t_1, denotes the time elapsed when 1_{SU} reaches 217.066 m, and time t_{58} denotes the time elapsed when 58_{SU} reaches the same depth. The table shows that it will take 503.21 seconds (t_1) for one SU to settle a length of 217.066 m. When 1_{SU} reaches 217.066 m it will take 2.52 seconds until 58_{SU} reaches the same depth. This is calculated from Eq. 57.

$$\Delta t = t_{58} - t_1 = 505.73s - 503.21s = 2.52\ s \qquad \text{Equation 57}$$

With one column of SUs sliding down the low-side of the blank pipe section it will take 505.73 seconds (t_{58}) to achieve the first layer of SUs. The remaining layers will use a time t_l, per layer, calculated from Eq. 58.

$$\begin{aligned} t_l &= \Delta t + t_a = (t_{58} - t_1) + t_a \\ &= (505.73s - 503.21s) + 0.021293\ s\ s \\ &= 2.54\ s \end{aligned} \qquad \text{Equation 58}$$

V_{OH-BP}	4.873512534	m^3	Length	229	m		
Volume occupied	0.253975755	m^3	Length occupied	11.93399	m		
Volume to pack	4.619536779	m^3	Length to fill	217.0660	m		
v_{SU}	25.88155718	m/min	Height of one layer	0.009865	m		
	0.431359286	m/s	Layers needed	22003.3			
			SU placement in relation to length of section, meters				
Seconds	1_{SU}		2_{SU}	3_{SU}	22.6_{SU}	23.6_{SU}	58_{SU}
1	0.43136		0.41231	0.39326	0.01905	0.00000	
2	0.86272		0.84367	0.82462	0.45041	0.43136	
3	1.29408		1.27503	1.25598	0.88177	0.86272	0.20823
4	1.72544		1.70639	1.68734	1.31313	1.29408	0.63959
5	2.15680		2.13775	2.11870	1.74449	1.72544	1.07095
6	2.58816		2.56911	2.55006	2.17585	2.15680	1.50231
7	3.01952		3.00047	2.98142	2.60721	2.58816	1.93367
8	3.45087		3.43182	3.41277	3.03857	3.01952	2.36502
t_1 503.21395	217.066		217.047	217.028	216.654	216.635	215.980
503.25811			217.066	217.047	216.673	216.654	216.000
503.30228				217.066	216.692	216.673	216.018
504.16979					217.066	217.047	216.393
504.21395						217.066	216.412
t_{58} 505.73123							217.066

Table 19: Position of nSU in blank pipe section after time t

With an increased number of columns with SUs sliding down the low-side of the blank pipe section will decrease the total packing time for the blank pipe section. Table 20 shows the amount of time it will take to pack the first layer, the remaining layers and the total packing time for 1-5, 11.66 and 16 columns of SUs. To avoid accumulation of gravel in the upper screen section is it

necessary for the SUs to settle and pack the well within the 80.6 minutes calculated in Eq. 51. From Table 20 can it be seen that with 11.66 columns of SUs this is achieved.

A maximum number of 16 SU columns can be placed in the well within the requirements presented in Section 5.2.2. Fig. 38 shows that 16 columns of SUs will cover the entire low-side of the blank pipe section. Table 20 shows that with 16 columns of SUs the entire blank pipe section will be packing in 58.7 minutes. With a pumping rate that use 80.6 minutes to pump the sufficient gravel needed into the well it will not be possible to achieve 16 columns of SUs; The gravel concentration pumped into the well is to low.

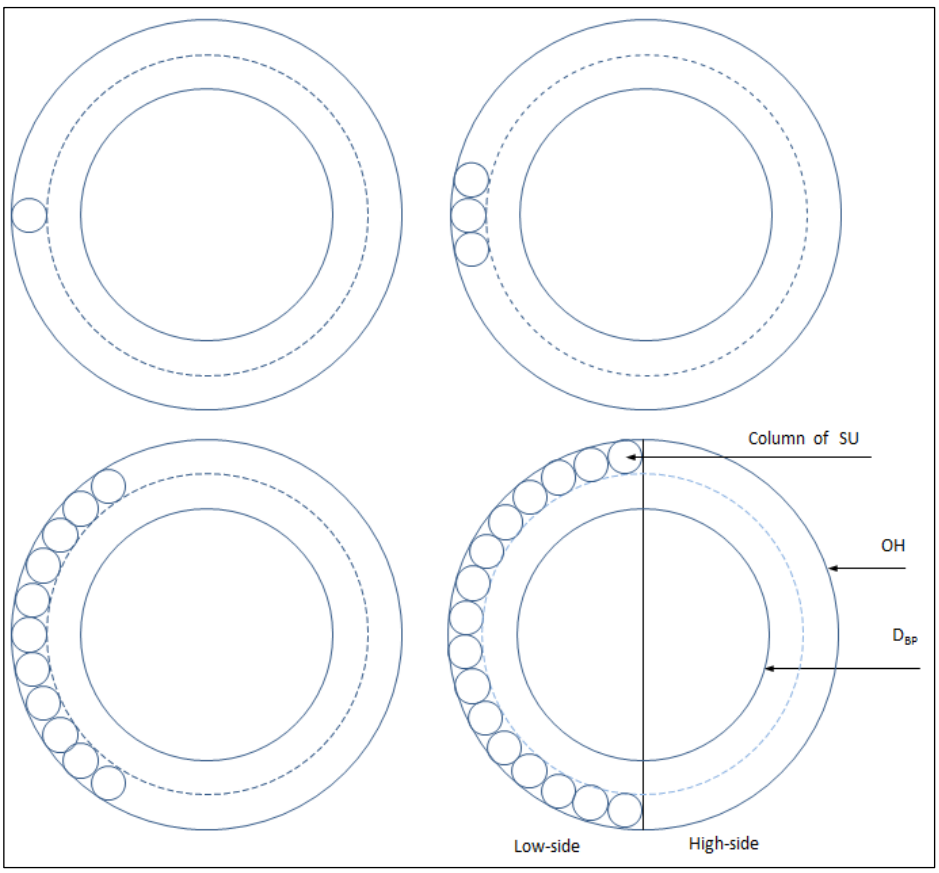

Figure 38: Columns of SUs placed on the low-side of the blank pipe section

Columns of SU	First layer	Remaining layers	SUs/Second	Total packing time
	Seconds	Seconds/Layer		Min
1	505.7312	2.5386	22.643532	939.3
2	252.8656	1.2693	45.287064	469.7
3	168.5771	0.8462	67.930596	313.1
4	126.4328	0.6346	90.574128	234.8
5	101.1462	0.5077	113.217660	187.9
11.66	43.3866	0.2178	263.941721	80.6
16	31.6082	0.1587	362.296513	58.7

Table 20: Columns of SUs with respective packing time

6.3.3 Optimized gravel concentration in relation to gravel settling in blank pipe section

From the calculations based on pump rate for the blank pipe section in Section 6.3.2.1 shows that with a pump rate Q_P, of 1.1 m^3/min and a gravel concentration $\dot{m}_g$, of 90 kg/m^3 it will take 80.6 minutes to pack the blank pipe section.

Table 20 shows that with 16 columns of SUs the packing time can be reduced to 58.7 minutes in the blank pipe section. In order to reduce the packing time a higher concentration of gravel is needed. Table 20 shows that 16 columns of SUs will give a rate of 362.3 SUs per second. This gives a new packing rate Q_p of 0.07869 m^3/min calculated from Eq. 59.

$$\begin{aligned} Q_p &= \frac{N_{SU}}{s} \cdot V_{SU} \\ &= 362.3\ \frac{SU}{s} \cdot\ 3.61979 \cdot 10^{-6}\,\frac{m^3}{SU} \\ &= 0.00131\ \frac{m^3}{s} \\ &= 0.07869\ \frac{m^3}{min} \end{aligned}$$ Equation 59

The new packing rate Q_p, of 0.07869 m^3/min gives a corresponding gravel concentration of 123.538 kg/min by combining Eq. 41 and Eq. 49 as shown in Eq. 60. These results show that an increase of gravel concentration from 90 kg/min to 123.537 kg/min in the modified well can be done without accumulation of gravel in the upper screen section.

$$\begin{aligned} \dot{m}_g &= Q_p \cdot\ V_{fg} \cdot \rho_g \\ &= 0.07869\ \frac{m^3}{min} \cdot\ 0.5793 \cdot 2710\ \frac{kg}{m^3} \\ &= 123.537\,\frac{kg}{min} \end{aligned}$$ Equation 60

Increasing the concentration of gravel from 90 kg/min to 123.537 kg/min will reduce the packing time in the blank pipe section with 21.9 minutes. This is calculated from Eq. 61, where T_{P90} denotes the packing time with a gravel concentration of 90 kg/min, and $T_{P123.537}$ denotes the packing time with a gravel concentration of 123.537 kg/min.

$$\begin{aligned} \Delta t &= T_{P90} - T_{P123.537} \\ &= 80.6\ min - 58.7\ min \\ &= 21.9\ \text{min} \end{aligned}$$ Equation 61

An overview of total pumping time in addition to the quantity gravel and slurry needed can be seen in Table 21 for a gravel concentration of 90 kg/min, and Table 22 for a gravel concentration of 123.537 kg/min.

From these two tables it can be seen that a gravel concentration of 90 kg/min results in a total pumping time of 152.9 minutes, and a gravel concentration of 123.537 kg/min results in a total

pumping time of 116.4 minutes. Eq. 62 shows that by increasing the gravel concentration from 90 kg/min to 123.537 kg/min will reduced the pumping time with 36.5 minutes. The pump time required to lift the remaining slurry in drillpipe after screenout is not included in these calculations.

Section		Cross sectional area	Length	Volume	Volume gravel	Volume slurry needed
		m^2	m	m^3	m^3	m^3
OH-Screen (Upper)	:	0.01776	80	1.42040	0.82289	27.2559
OH-Screen (Lower)	:	0.01776	80	1.42040	0.82289	27.2559
OH-BP	:	0.02128	229	4.87351	2.82340	93.5173
Drillpipe	:	0.00924	2,182	20.1588	0.60862	20.1588
Total	:			**27.873**	**5.0778**	**168.188**

Where					
Gravel conc.	90	kg/min	**Pumping time**		
Gravel density	2,710	kg/m^3	152.9	min	
Gravel fraction	0.03321	m^3 Gravel / m^3 Slurry	2.548	hours	
	81.82	kg Gravel / m^3 Slurry			
Slurry rate	1.1	m^3/min			

Table 21: Data for gravel concentration of 90 kg/m^3

Section		Cross sectional area	Length	Volume	Volume gravel	Volume slurry needed
		m^2	m	m^3	m^3	m^3
OH-Screen (Upper)	:	0.01776	80	1.42040	0.82289	19.8566
OH-Screen (Lower)	:	0.01776	80	1.42040	0.82289	19.8566
OH-BP	:	0.02128	229	4.87351	2.82340	68.1296
Drillpipe	:	0.00924	2,182	20.1588	0.83541	20.1588
Total	:			**27.873**	**5.3046**	**128.002**

Where						
Gravel conc.	:	123.537	kg/min	**Pumping time**		
Gravel density	:	2,710	kg/m^3	116.4	min	
Gravel fraction	:	0.04144	m^3 Gravel / m^3 Slurry	1.939	hours	
	:	112.31	kg Gravel / m^3 Slurry			
Slurry rate	:	1.1	m^3/min			

Table 22: Data for gravel concentration of 123.537 kg/min

$$\begin{aligned}\Delta t &= T_{P90} - T_{P123.537} \\ &= 152.9\ min - 116.4\ min \\ &= 36.5\ \text{min}\end{aligned}$$

Equation 62

7. CONCLUSION AND FURTHER WORK

A thorough work has been done finding a settling velocity that applies for gravel in an inclined/nearly vertical regime with Newtonian fluids. Several velocity theorems have been investigated and calculated.

By investigating how the gravel settles in an OHGP with a near vertical regime it has been shown in this thesis that an optimization of the gravel concentration can be calculated. Applying the optimized gravel concentration will ensure a fully packed blank pipe section without accumulation of gravel in overlying screens. For a specific pump rate, this gravel concentration will keep the pumping time at a minimum. Keeping the pumping time at a minimum will reduce the completion cost in terms of expensive rig-time and is therefore beneficial to the oil and gas industry.

The main parameters affecting the optimization of gravel concentration are based on gravel settling velocity in blank pipe sections, properties of the SUs and well geometry.

Optimizing the gravel concentration in the well presented in this thesis reduced the pumping time from 152.9 minutes to 116.4 minutes, this by calculating the settling velocity of the SUs in the inclined blank pipe section.

Gravel settling and placement in nearly vertical blank pipe section is different from placement and settling of gravel in completely vertical blank pipe section. The Boycott effect that occurs in the inclined blank pipe section will due to density differences and inclination result in a greater settling velocity as the falling gravel and the rising fluid get out of each other's way.

Calculations applied in this thesis have been carried out with several assumptions and should be tested experimental. Simple experiments with solid spheres sliding down an inclined tube submerged in a Newtonian liquid can be compared to the equations applied in this thesis. With a high-speed camera and colorized gravel, knowledge of gravel settling and placement can be obtained in a laboratory gravel pack scale model. This will give a greater knowledge of the velocity acceleration that has been neglected in this thesis.

8. REFERENCES

1. Oilfield Wiki, *Sand control*, http://www.oilfieldwiki.com/wiki/Sand_control, [Accessed 15.04 2014].

2. Halliburton Energy Services Inc., 2007, *Sand Control Completions,* unpublished internal document.

3. Kaarigstad, H., Strachan, C., Fjellstad, V., Gyland, K.R. and Filbrandt, J., 2014, "Qualification of Gravel Packing in HP/HT Wells", paper SPE -168210-MS presented at the SPE International Symposium and Exhibition on Formation Damage Control, Lafayette, Louisiana, USA, 26-28 February.

4. Ott, W.K. and Woods, J.D., 2005, *Modern sandface completion practices handbook*, World Oil, Houston.

5. Matanovic, D., Cikes, M. and Moslavac, B., 2012, *Sand control in well construction and operation*, Springer, Dordrecht.

6. Allen, T.O. and Roberts, A.P., 1989, *Production operations* (Vol. 2), Oil & Gas Consultants International, Tulsa.

7. Han, G., Dusseault, M.B. and Cook, J., 2004, "Why Sand Fails After Water Breakthrough", paper ARMA-04-505 presented at the Gulf rocks 2004, the 6th North America Rock Mechanics Symposium (NARMS): Rock Mechanics Across Borders and Disciplines, Houston, Texas, U.S.A., 5-9 June.

8. Kalnæs, P.E., 2013, *Sand Control: Gravel Packing,* unpublished internal document, Halliburton.

9. Ammonite Corrosion Engineering Inc., *Degradation Mechnisms Library*, http://www.ammonite-corrosion.com/degrade.html, [Accessed 17.04 2014].

10. Penberthy, W.L. and Shaughnessy, C.M., 1992, *Sand control*, Henry L. Doherty Memorial Fund of AIME, Society of Petroleum Engineers, Richardson, Texas.

11. Cholet, H., 2000, *Well production practical handbook*, Éditions technip, Paris.

12. Bellarby, J., 2009, *Well completion design*, Elsevier, Amsterdam.

13. Penberthy, W.L. and Echols, E.E., 1993, Gravel Placement in Wells, *Journal of Petroluem Technology*, **45**, pp. 612-674.

14. Costamte, Y.R., 2010, *Modeling of Open-Hole Gravel Packing on Longer Blank Pipe and Screen Sections*, MSc. thesis, University of Stavanger, Norway.

15. DuneFront, *Resources*, http://dunefront.com/resources.aspx, [Accessed 15.04 2014].

16. QAQC Lab, *Equipment for quality control and r&d applications*, http://www.qclabequipment.com/AggregateSifting.html, [Accessed 20.02 2014].

17. Rhodes, M. J., 2008, *Introduction to Particle Technology*, Wiley, Chichester, England.

18. Zwolle, S. and Davies, D.R., 1983, Gravel Packing sand Quality - A Quantitative Study, *Journal of Petroleum Technology*, **35**, pp. 1,042-1,050.

19. Weatherford, *Gravel Pack Systems*, http://www.weatherford.com/dn/wft193884, [Accessed 25.04 2014].

20. American Petroleum Insitute, *Recommended Practices for Testing Sand Used in Gravel Packing Operations*, API Recommended Practice 58,1995

21. Mader, D., 1989, *Hydraulic Proppant Fracturing and Gravel Packing*, Elsevier, Amsterdam.

22. CARBO Ceramics, *Carobolite*, http://www.carboceramics.com/attachments/wysiwyg/23/1001_68_C_Lite_ts_Lr(4).pdf, [Accessed 15.04 2014].

23. Boulet, D.P., 1979, Gravel for Sand Control: A Study of Quality Control, *Journal of Petroleum Technology*, **31**, pp. 164-168.

24. SPE, *History of gravel packs*, http://petrowiki.org/History_of_gravel_packs, [Accessed 02.05. 2014].

25. Parlar, M. and Albino, E.H., 2000, Challenges, Accomplishments, and Recent Developments in Gravel Packing, *Journal of Petroleum Technology*, **52**, pp. 50-58.

26. Omland, T.H., 2009, *Particle settling in non-Newtonian drilling fluids*, PhD. thesis, University of Stavanger, Norway.

27. Pattillo, Chris, *Inclined Settlers*, http://www.rpi.edu/dept/chem-eng/biotech-Environ/SEDIMENT/boycott.htm, [Accessed 19.03 2014].

28. Indian Institute of Technology, *Batch Settling of Solids Slurries*, http://www.che.iitb.ac.in/courses/uglab/cl333n335/fm304-settling.pdf, [Accessed 19.03 2014].

29. Calvert, D.G., Heathman, J.F. and Griffith, J.E., 2000, Study reveals variables that affect cement-plug stability, *Oil & Gas Journal*, **98**(8), pp. 54-62.

30. Paslay, P.R., Sathuvalli, U.B. and Payne, M.L., 2007, "A Phenomenological Approach to Analysis of Barite Sag in Drilling Muds", paper SPE- 110404 presented at the SPE Annual Technical Conference and Exhibition, Anaheim, California, U.S.A., 11-14 November.

31. Calvert, D.G., Heatherman, J.F. and Griffith, J.E., 1995, "Plug Cementing: Horizontal to Vertical Conditions", paper SPE-30514-MS presented at the SPE Annual Technical Conference and Exhibition, Dallas, Texas, U.S.A., 22-25 October.

32. Bahadori, A., Nwaoha, C. and Clark, M.W., 2013, *Dictionary of Oil, Gas, and Petrochemical Processing*, Taylor & Francis, Boca Raton.

33. Schlumberger, *Rat Hole*, http://www.glossary.oilfield.slb.com/en/Terms.aspx?LookIn=term name&filter=rathole, [Accessed 08.06 2014].

34. Serene Energy, *Top Set Open Hole Gravel Pack*, http://www.i.sereneenergy.org/i/Top-Set-Open-Hole-Gravel-Pack.html, [Accessed 21.05 2014].

35. Brill, J.P., Mukherjee, H. , 1999, *Multiphase Flow in Wells*, Society of Petroleum Engineers Inc., Richardson, Texas.

36. Selker, J.S., McCord, J.T. and Keller, C.K., 1999, *Vadose zone processes*, CRC Press, Boca Raton.

37. Spitzer, D.W., 2001, *Flow Measurement: Practical Guides for Measurement and Control* (2 ed.), The International Society of Automation, Research Triangle Park, North Carolina.

38. Takács, G., 2005, *Gas Lift Manual*, PennWell Corporation, Tulsa, Oklahoma.

39. Wikipedia, *Hydraulic diameter*, http://en.wikipedia.org/wiki/Hydraulic_diameter, [Accessed 12.04 2014].

40. Wikipedia, *Stokes' law*, http://www.en.wikipedia.org/wiki/Stokes'_law, [Accessed 14.03 2014].

41. Wikipedia, *Terminal velocity*, http://en.wikipedia.org/wiki/Terminal_velocity, [Accessed 08.06 2014].

42. *Partikkeltransport i vertikale annuli,* lecture notes distributed in BIP200 Bore og brønnvæsker at The University of Stavanger, spring 2012.

43. Saasen, A., 2002, "Sag of Weight Materials in Oil Based Drilling Fluids", paper IADC/SPE 77190 presented at the IADC/SPE Asia Pacific Drilling Technology presentation, Jakrata, Indonesia, 9-11 September.

44. Jalaal, M. and Ganji, D.D., 2011, On unsteady rolling motion of spheres in inclined tubes filled with incompressible Newtonian fluids, *Advanced Powder Technology*, **22**(1), pp. 58-67.

45. Jalaal, M. and Ganji, D.D., 2010, An analytical study on motion of a sphere rolling down an inclined plane submerged in a Newtonian fluid, *Powder Technology*, **198**(1), pp. 82-92.

46. Chhabra, R.P., Kumar, M. and Prasad, R., 2000, Drag on spheres in rolling motion in inclined smooth tubes filled with incompressible liquids, *Powder Technology*, **113**(1–2), pp. 114-118.

47. Hodne, H., Galta, S. and Saasen, A., 2007, Rheological modelling of cementitious materials using the Quemada model, *Cement and Concrete Research*, **37**(4), pp. 543-550.

48. Quemada, D., 1998, Rheological modelling of complex fluids. I. The concept of effective volume fraction revisited, *The European Physical Journal -Applied Physics*, **1**(01), pp. 119-127.

49. Çengel, Y.A. and Cimbala, J.M., 2006, *Fluid Mechanics: Fundamentals and applications*, McGraw-Hill, New York.

50. Wikipedia, *Reynolds number*, http://en.wikipedia.org/wiki/Reynolds_number, [Accessed 09.05. 2014].

51. Beggs, H.D, 2003, *Production Optimization Using Nodal TM Analysis*, OGCI and Petroskills Publications, Tulsa, Oklahoma.

52. Colebrook, C.F., 1939, Turbulent flow in pipes, with particular reference to the transition region between smooth and rough pipe laws, *Journal of the Institution of Civil Engineers*, **11**, pp. 133-156.

53. Buzzelli, D., 2008, Calculating friction in one step, *Machine Design*, **80**, pp. 54-55.

54. Winning, H.K., and Coole, T., 2013, Explicit Friction Factor Accuracy and Computational Efficiency for Turbulent Flow in Pipes, *Flow Turbulence Combust*, **90**(1), pp. 1-27.

55. Moody, L.F., 1944, Friction Factors for Pipe Flow, *Transactions of the ASME*, **66**, pp. 671-684.